# A Belief Rule-Based Expert System for Fault Diagnosis of Marine Diesel Engines

Xiaojian Xu, Xinping Yan, Chenxing Sheng, Chengqing Yuan, Dongling Xu, and Jianbo Yang

***Abstract*—This paper proposes a new belief rule-based (BRB) expert system for fault diagnosis of marine diesel engines. The expert system is the first of its kind that consists of multiple concurrently activated BRB subsystems, in which each subsystem has its distinctive outputs and uses the evidential reasoning approach for inference. This novel modeling approach can be applied to identify fault modes that may co-exist. In essence, the group of BRB subsystems is used to model the nonlinear relationships between the fault features and the fault modes in marine diesel engines. The initial BRB expert system can be established by using expert experience and then optimized by using the data samples accumulated during the operation of marine diesel engines. Due to limitations in knowledge and data collected, ignorance is also considered in some BRB subsystems. The proposed BRB expert system is applied to abnormal wear detection for a kind of marine diesel engine. The performance of the BRB expert system is investigated in comparison with that of artificial neural network (ANN) models, support vector machine (SVM) models, and binary logistic regression model with fivefold cross-validation. The results show that the BRB expert system can be used for fault diagnosis of marine diesel engines in a probabilistic manner, which outperforms the ANN models, SVM models, and the binary logistic regression model in terms of accuracy and stability, and can effectively identify concurrent faults.**

***Index Terms*—Diesel engines, expert systems, fault diagnosis, marine vehicle power systems, wear.**

Manuscript received November 3, 2016; accepted September 19, 2017. This work was supported in part by the EU FP7 Marie Curie IRSES project under Grant EC-GPF-314836, in part by the National Science Foundation of China under Grant 51422507, in part by the Innovation Groups Project of Hubei Province Natural Science Foundation under Grant 2013CFA007, and in part by the U.S. Air Force Office of Scientific Research under Grant FA2386-15-1-5004. This paper was recommended by Associate Editor G. Provan. *(Corresponding author: Xinping Yan.)*

X. Xu is with the Reliability Engineering Institute, National Engineering Research Center for Water Transport Safety, Wuhan University of Technology, Wuhan 430063, China, and also with the Decision and Cognitive Sciences Research Centre, University of Manchester, Manchester M15 6PB, U.K. (e-mail: xuxiaojian880303@163.com).

X. Yan, C. Sheng, and C. Yuan are with the Reliability Engineering Institute, National Engineering Research Center for Water Transport Safety, Wuhan University of Technology, Wuhan 430063, China (e-mail: xpyan@whut.edu.cn; scx01@126.com; ycq@whut.edu.cn).

D. Xu and J. Yang are with Decision and Cognitive Sciences Research Centre, University of Manchester, Manchester M15 6PB, U.K. (e-mail: ling.xu@manchester.ac.uk; jian-bo.yang@manchester.ac.uk).

This paper has supplementary downloadable material available at http://ieeexplore.ieee.org, provided by the authors. This includes a PDF of the dataset used for model training and testing. This material is 0.182 MB in size.

Color versions of one or more of the figures in this paper are available online at http://ieeexplore.ieee.org.

Digital Object Identifier 10.1109/TSMC.2017.2759026

## I. Introduction

CURRENTLY most ships are propelled by diesel engines, and faults in marine diesel engines have great influence on the normal operation of ships. As indicated in the report of Swedish Club on main engine damage, claims caused by marine diesel engine damage account for 37.7% of the total ship machinery claims during the period from 2005 to 2011, leading to over $20 million U.S. loss [1]. Consequently, it is necessary to pay more attention to the fault diagnosis of marine diesel engines to improve their reliability.

With expert experience and fault data collected during engines' operation, faults in engines can be identified by fault diagnostic models. Automatic fault diagnosis is an artificial intelligence problem and a variety of intelligent algorithms have been applied in this area. Among these methods, rule-based expert system is one of the most widely used methods. By using a variety of condition monitoring information, such as vibration signal, instantaneous angular speed signal, performance parameters, and oil information, expert systems can provide diagnostic advice automatically to ensure the safe running of machines [2]–[5]. Currently, simple diagnostic systems embedded in condition monitoring systems onboard are still mainly based on traditional rule-based expert systems. However, limited knowledge acquisition is the bottle neck of traditional rule-based expert system, limiting its application scope. Meanwhile, traditional rule-based expert systems for fault diagnosis lack flexibility. Once an expert system is built, it cannot learn from real operating data or make adjustments to meet changing environments.

To better describe the nonlinear relationship between fault features and fault modes, intelligent algorithms with strong computing, nonlinear mapping and self-learning capabilities have been used in fault diagnosis. Artificial neural network (ANN) is the most representative among these methods. Fault diagnosis systems based on ANN were developed to detect engines' combustion fault, wear fault, fuel injection fault, etc. [6]–[10]. But an ANN model is a black-box simulator in the sense that the relationship between the inputs and outputs of the model is difficult to be explained. Perturbation to the inputs of neural networks could affect their stability, reducing the robustness of ANN models [11]. Additionally, an important but difficult problem for ANN is to determine its structure. For example, the performance of a neural network will be different with the variation of the number of hidden units [12].

Other methods, such as support vector machine (SVM) [13], grey target theory [14], Dempster–Shafer (D–S) theory of

evidence [15], statistic method [16], etc. are also used for fault diagnosis of engines. A common concern on the above-mentioned methods is that they cannot take full advantages of quantitative and qualitative information simultaneously. For example, a traditional rule-based expert system cannot be trained; models constructed with intelligent algorithms like ANN can be trained using quantitative information only but lack the ability of accommodating expert knowledge.

The belief rule-based (BRB) inference methodology is proposed to analyze the complex decision problems with both quantitative and qualitative information [17]–[19]. It is developed on the basis of D–S theory of evidence, decision theory and traditional "IF-THEN" rules [18]. Different from traditional IF-THEN rules, each consequent attribute of a belief rule is associated with a belief degree. Experts can use their subjective knowledge to build an initial BRB model. The parameters of the BRB model can be optimized using numerical data to describe the nonlinear relationship between inputs and outputs more accurately [19]. The parameters of the BRB model can also be adjusted by experts using their experiences and knowledge as the belief rules are transparent and interpretable [20]. The BRB inference methodology has been applied in financial decision-making, medical care, oil leakage detection, product life estimation, etc. [17], [21]–[23]. It has also been used in marine domain, such as accident analysis, technique selection for ship emission reduction, and marine security assessment [24]–[26]. In the fault diagnostic area, BRB inference methodology is used to detect the track vertical irregularity of trains [27], and fault diagnosis of aircraft navigation systems [28]. However, no research shows that the BRB inference methodology has been applied to fault diagnosis in ships.

From the literature review, it can be found that in the previous research the states of consequent attributes in a BRB model are required to be mutually exclusive with each other. However, fault diagnosis, especially fault mode identification in ships has its own characteristics which needs to be taken into account when BRB and evidential reasoning (ER) approaches are used for causal inference. First, fault modes generally are not mutually exclusive, but are coupled with each other in the sense that the occurrence of one fault may lead to another fault mode [29]. Moreover, different types of faults may occur simultaneously. As a result, when fault modes are used as consequent attributes in a BRB model, all combinations of concurrent fault modes should be considered to make a BRB model logical. Second, there is a many-to-many relationship between fault features and fault modes, which means that one fault symptom can be caused by several different fault modes and vice versa. In the previous fault diagnostic models, different fault modes were considered to be exclusive with each other and the combinations of different fault modes were ignored, and therefore the fault diagnostic models only generated a single output and were not suitable for concurrent fault modes. Additionally, all fault modes shared the same fault features as the input of fault diagnostic models, which increased the model complexity, especially in the occasion that a large number of fault features were considered. For example, Zhang *et al.* [30] used different fault modes to construct a BRB model for fault diagnosis in engines, but the fault modes were considered to be exclusive and concurrent faults were ignored in the model.

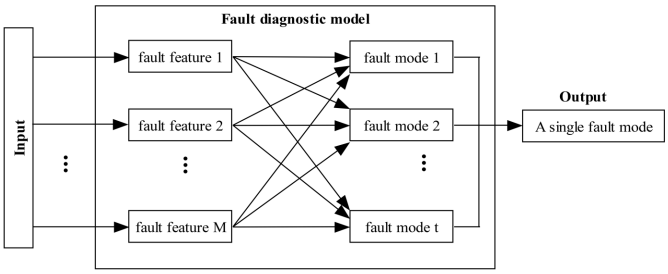


Fig. 1. Fault diagnostic model for a single fault.

Based on the above analysis, a new fault diagnostic model structure is proposed in this paper to solve the problems in the previous fault diagnostic models. BRB inference methodology is used to link the fault modes of marine diesel engines with their fault features. A case for detecting abnormal wear of a kind of marine diesel engine is examined using the new BRB fault diagnostic model to show its potential in wide application. With fivefold cross-validation, the performance of the BRB fault diagnostic model is compared with that of the ANN model, the SVM model, and the binary logistic regression model.

## II. Fault Diagnostic Model Based on BRB Inference Methodology

### A. Model Structure

One of the most commonly employed fault diagnostic model is for single fault diagnosis as illustrated in Fig. 1. The relationship between fault features and different fault modes is built by an algorithm, such as statistical methodology, ANN, or SVM, which is the basis of fault diagnosis. As shown in Fig. 1, every fault mode shares the same fault feature vector, and $t$ single fault modes compose the fault frame of discernment $\Theta = \{F_1, F_2, \ldots, F_t\}$, which is a finite nonempty exhaustive set of all possible failure hypotheses $F_i (i = 1, 2, \ldots, t)$. Given the inputs about the $M$ fault features for the fault diagnostic model, the model can generate a single output based on the relationship between the $M$ fault features and $t$ fault modes, identifying which fault mode is true. The fault diagnostic model in Fig. 1 can only identify a single fault mode at a time and is not appropriate for the concurrent fault diagnosis of multiple modes. As mentioned in Section I, there are a variety of fault modes in marine diesel engines, some of which may co-exist simultaneously, and the above single fault diagnostic model is not applicable in this case.

To construct a fault diagnostic model for identification of multiple concurrent fault modes, all combinations of failure hypotheses $F_i$ in $\Theta$ should be considered. In other word, $\Omega(\Theta) = \{F_1, \ldots, F_t, \{F_1, F_2\}, \ldots, \{F_1, \ldots, F_i\}, \ldots, \Theta\}$ should be used as the fault frame of discernment, consisting of $2^t - 1$ subsets of $\Theta$ [31]. As shown in Fig. 2, the relationship between $M$ fault features and $2^t - 1$ fault modes (including $t$ single fault modes and $2^t - t - 1$ multiple concurrent fault modes) is the basis of multiple concurrent fault

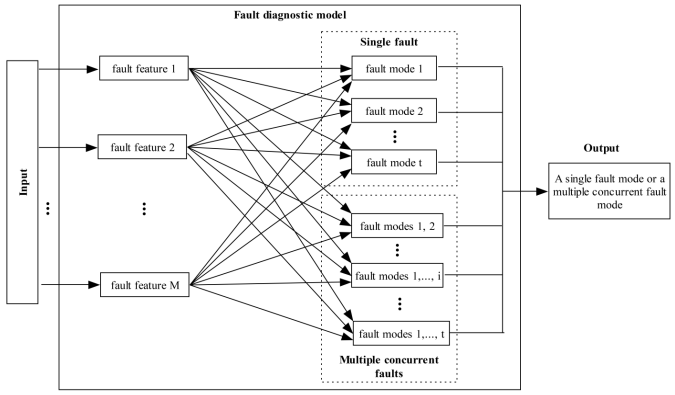


Fig. 2. Fault diagnostic model for multiple concurrent fault modes in an integral structure.

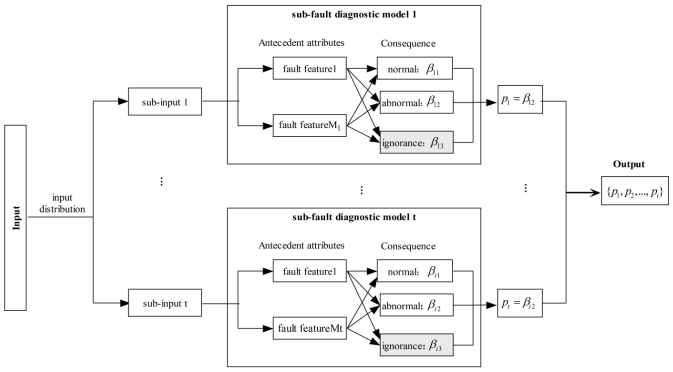


Fig. 3. Fault diagnostic model for multiple concurrent fault modes in a parallel structure.

diagnosis. Given input to a fault diagnostic model as shown in Fig. 2, it will generate a single fault mode or a combination of multiple concurrent fault modes as output. However, there are several inherent problems in this model structure.

1) It is difficult to determine a fault feature vector for multiple concurrent fault modes, and therefore the relationship between fault features and fault modes is hard to be determined.
2) With the increase of failure hypotheses considered in the fault diagnostic model, the number of combinations of different fault modes will rise exponentially. When fault samples are insufficient and cannot cover all fault modes, a fault diagnostic model proposed may not be reliable.

To deal with the above problems, a new parallel fault diagnostic model is proposed as shown in Fig. 3, which contains $t$ parallel subfault diagnostic models for $t$ single fault modes. Each submodel corresponds to one particular fault mode and has its own fault features. Due to the many-to-many relationship between fault features and fault modes, different submodels may share the same fault feature. The output of each subfault diagnostic model are the belief degrees of two states which are normal and abnormal, where normal means this fault does not occur and abnormal indicates this fault occurs. The input coming into the fault diagnostic model will be distributed to every submodel according to its fault features. The belief degrees of the two states (normal and abnormal) of a fault mode are generated by the corresponding submodel, represented by $\beta_{hi}(i = 1, 2; h = 1, 2, \ldots, t)$, where $h$ is the $h$th subfault diagnostic model. The subfault diagnostic models do not affected each other and the final diagnostic result $\{p_1, p_2, \ldots, p_h, \ldots, p_t\}$ is composed of the results generated by each submodel, where $p_h$ equals the belief degree of the abnormal state in the $h$th fault mode, i.e., $p_h = \beta_{h2}(h = 1, 2, \ldots, t)$.

Currently, most fault diagnostic models are still about single fault diagnosis, ignoring concurrent faults, especially in marine fault diagnosis. Compared with models in Figs. 1 and 2, the fault diagnostic model in Fig. 3 is well suited for concurrent fault diagnosis of multiple modes which is transformed into several parallel binary classification problems in the one-versus-all scheme [32]. Instead of using all combinations of failure hypotheses as outputs of a fault diagnostic model directly, the number of parameters of the diagnostic model in Fig. 3 decreases significantly, reducing the complexity of the model. Since each submodel in Fig. 3 has its own fault features rather than sharing whole fault features for all fault modes, the complexity of the diagnostic model can also be reduced and the relationship between input and output can be described more clearly. Additionally, the fault diagnostic model in Fig. 3 is easier to be expanded due to the parallel structure. When a new fault mode is added into the diagnostic model, only a submodel for the new fault mode needs to be constructed and tuned without modifying the other submodels. However, the model either in Figs. 1 or 2 has to be reconstructed totally including the inputs, outputs and the relationships between fault features and fault modes.

In order to use the qualitative and quantitative information simultaneously, BRB inference methodology is applied to establish the relationship between the fault features and fault modes in every subfault diagnostic model. The development of the BRB expert system for fault diagnosis of marine diesel engines includes belief rule base construction, transformation of fault feature data, rule inference, model optimization, and final diagnostic result generation.

### *B. Belief Rule Base*

In the BRB inference methodology, the $k$th belief rule in the BRB subsystem for the $h$th $(h = 1, 2, \ldots, t)$ fault mode is defined as follows [18]:

$$
\begin{aligned}
&R_{hk}:\\
&\quad \text{IF: } X_{h1} \text{ is } A^k_{h1j} \wedge X_{h2} \text{ is } A^k_{h2j} \wedge \cdots \wedge X_{hM_h} \text{ is } A^k_{hM_hj}\\
&\text{THEN:}\\
&\quad \left\{\left(D_{h1}, \beta^k_{h1}\right), \left(D_{h2}, \beta^k_{h2}\right), \ldots, \left(D_{hN_h}, \beta^k_{hN_h}\right)\right\}\\
&\qquad \left(\sum_{n=1}^{N_h} \beta^k_{hn} \le 1\right)(n = 1, \ldots, N_h).
\end{aligned}
$$

In the rule, $X_{hi}(i = 1, 2, \ldots, M_h)$ is the $i$th fault feature which is used as an antecedent attribute of the $k$th belief rule. $A^k_{hij}(i = 1, 2, \ldots, M_h; j = 1, 2, \ldots, T_{hi})$ denotes the referential value of the $i$th fault feature, where $M_h$ is the number of fault features and it varies with the different BRB subsystems

because each fault mode has its own fault features; $T_{hi}$ is the number of referential points used for the $i$th fault feature and the number of referential points for each fault feature can be either the same or different, depending on the need of the real problems. $M_h$ and $T_{hi}(i = 1, 2, \ldots, M_h)$ have direct influences on the complexity of the $h$th BRB subsystem and determine the number of rules in the belief rule base which is $\prod_{i=1}^{M_h} T_{hi}$.

$D_{hn}(n = 1, 2, \ldots, N_h)$ is the consequent state for the $h$th fault mode with the belief degree $\beta_{hn}^k$, where $N_h$ is the number of consequent states. In the fault diagnostic model shown in Fig. 3, $N_h$ mostly equals two and the consequent states include *normal* and *abnormal*. If the sum of the belief degrees $\beta_{hn}^k(n = 1, 2, \ldots, N_h)$ for the consequence of the $k$th belief rule is one, the belief rule will be said to be complete; otherwise it is incomplete and the remaining belief degree is referred to ignorance as indicated by the gray box in Fig. 3. Generally, ignorance is expressed by the power set of a set of mutually exclusive and collectively exhaustive consequent states. For example, ignorance in the BRB subsystem in Fig. 3 is {*normal*, *abnormal*}. During the construction of the BRB subsystem for fault diagnosis, some measures should be taken to eliminate or reduce the ignorance of consequent states, such as adding a new antecedent attribute, but if the ignorance cannot be eliminated, it should be considered in the BRB subsystems. It is believed that the fault diagnostic result with ignorance is better than a misleading or a totally wrong fault diagnostic result.

In the $k$th rule of the $h$th BRB subsystem, $\theta_{hk}(k = 1, 2, \ldots, L_h)$ is the rule weight of the $k$th rule, indicating the importance of the $k$th rule in the $h$th BRB subsystem, and $L_h$ represents the number of rules in this subsystem; the antecedent attribute weights are $\delta_{hi}^k(i = 1, 2, \ldots, M_h)$. An initial BRB is constructed based on experts' subjective knowledge. Rule weights $\theta_{hk}(k = 1, 2, \ldots, L_h)$ and the weights of antecedent attributes $\delta_{hi}^k(i = 1, 2, \ldots, M_h)$ need to be determined, which are all set to be 1 initially in this paper. As for the belief degrees of consequent states, they are determined by the statistics of the whole historical operating data of marine diesel engines and the domain knowledge of experts.

### C. Transformation of Fault Data

The antecedent attributes of a BRB model in this paper are qualitative, and the quantitative fault feature data $x_{hi}$ should be transformed into belief degrees with the piecewise linear function. When $u(A_{hij}) \le x_{hi} \le u(A_{hij+1})$, $x_{hi}$ is transformed according to [33]

$$\alpha_{hij} = \frac{u\big(A_{hij+1}\big) - x_{hi}}{u\big(A_{hij+1}\big) - u\big(A_{hij}\big)}$$
$$\alpha_{hij+1} = \frac{x_{hi} - u\big(A_{hij}\big)}{u\big(A_{hij+1}\big) - u\big(A_{hij}\big)} \tag{1}$$

where $A_{hij}(i = 1, 2 \ldots, M_h; j = 1, 2, \ldots, T_{hi})$ is the referential points defined for antecedent attribute $X_{hi}(i = 1, 2, \ldots, M_h)$. $u(A_{hij})$ is the quantified value of $A_{hij}$ and $u(A_{hi1}) < u(A_{hi2}) < \cdots < u(A_{hiT_{hi}})$. After data transformation, the fault feature data $x_{hi}$ can be represented by $\{(A_{hi1}, 0), \ldots, (A_{hij-1}, 0), (A_{hij}, \alpha_{hij}), (A_{hij+1}, \alpha_{hij+1}), (A_{hij+2}, 0), \ldots, (A_{hiT_{hi}}, 0)\}$.

### D. Rule Inference

*1) Rule Activation:* $\alpha_{hi}^k \in \{\alpha_{hi1}, \ldots, \alpha_{hiT_{hi}}\}(i = 1, \ldots, M_h)$ acquired by (1) represent the extents to which each antecedent attribute of the $k$th belief rule is matched by the input data $x_h = \{x_{h1}, \ldots, x_{hM_h}\}$. $\cdot \prod_{i=1}^{M_h} (\alpha_{hij}^k)^{\bar{\delta}_{hi}^k}$ is the overall degree to which the $k$th rule is matched, where $\bar{\delta}_{hi}^k = \delta_{hi}^k / \max_{i=1,2,\ldots,M_h}\{\delta_{hi}^k\}$ is the relative weight of $X_{hi}(i = 1, 2, \ldots, M_h)$. The activation weight of the $k$th rule $\omega_{hk}$ is calculated from (2), which indicates the degree that the belief rule is activated. The more similarity between the antecedent attributes and the input fault feature data, the higher activation weight will be given to the rules. If $\omega_{hk}$ is zero, this rule will not be activated

$$\omega_{hk} = \frac{\theta_{hk}\left[\prod_{i=1}^{M_h}\left(\alpha_{hij}^k\right)^{\bar{\delta}_{hi}^k}\right]}{\sum_{l=1}^{L_h}\theta_{hl}\left[\prod_{i=1}^{M_h}\left(\alpha_{hij}^k\right)^{\bar{\delta}_{hi}}\right]}. \tag{2}$$

*2) Aggregation of Activated Rules:* The ER approach is applied to combine activated rules and generate final conclusions in the BRB inference. The activation weights acquired from (2) are treated as the relative importance of each consequence and the consequences generated by all the activated belief rules are aggregated by

$$\beta_{hj} = \frac{\mu\left[\prod_{k=1}^{L_h}\left(\omega_{hk}\beta_{hj}^k + 1 - \omega_{hk}\sum_{j=1}^{N_h}\beta_{hj}^k\right) - \prod_{k=1}^{L_h}\left(1 - \omega_{hk}\sum_{j=1}^{N_h}\beta_{hj}^k\right)\right]}{1 - \mu\left[\prod_{k=1}^{L_h}(1 - \omega_{hk})\right]} \times (j = 1, 2, \ldots, N_h) \tag{3}$$

$$\mu = \left[\sum_{j=1}^{N_h}\prod_{k=1}^{L_h}\left(\omega_{hk}\beta_{hj}^k + 1 - \omega_{hk}\sum_{j=1}^{N_h}\beta_{hj}^k\right) - (N_h - 1)\prod_{k=1}^{L_h}\left(1 - \omega_{hk}\sum_{j=1}^{N_h}\beta_{hj}^k\right)\right]^{-1} \tag{4}$$

where $\beta_{hj}$ is the predicted belief degree of the $j$th consequent state and the final conclusion $D_h$ can be expressed as follows:

$$D_h = \big\{\big(D_{hj}, \beta_{hj}\big), j = 1, \ldots, N_h\big\}. \tag{5}$$

### E. Optimization of BRB Model

The performance of the BRB system can be improved if the parameters of the BRB model are optimized using the operating data of marine diesel engines. The parameters of a BRB model that can be optimized include rule weights $\theta_{hk}(k = 1, 2, \ldots, L_h)$, antecedent attribute weight $\delta_{hi}^k(i = 1, 2, \ldots, M_h)$, and the belief degree of consequents $\beta_{hn}^k(n = 1, 2, \ldots, N_h)$.

In a BRB submodel for one fault mode, the outputs of the model are belief distributions as expressed by (5), and therefore the objective function of the optimization model is constructed as follows [19]:

$$\min_{P_h}\max_{\{\xi_j\}} \quad \big\{\xi_j(P_h), j = 1, \ldots, N_h\big\}$$
$$\xi_j = \frac{1}{S}\sum_{s=1}^{S}\Big(\beta_{hj}(s) - \hat{\beta}_{hj}(s)\Big)^2 (j = 1, \ldots, N_h) \tag{6}$$
$$\text{Subject to} \quad 0 \le \theta_{hk} \le 1, (k = 1, \ldots, L_h) \tag{6a}$$

$$0 \le \delta_{hi} \le 1, (i = 1, \ldots, M_h) \tag{6b}$$

$$0 \le \beta_{hj}^{k} \le 1, (j = 1, \ldots, N_h) \tag{6c}$$

$$\sum_{j=1}^{N_h} \beta_{hj}^{k} = 1 \tag{6d}$$

where $P_h = [\theta_{h1}, \ldots, \theta_{hL_h}, \delta_{h1}, \ldots, \delta_{hM_h}, \beta_{h1}, \ldots, \beta_{hN_h}]^T$ is the vector of the parameters which should be optimized in the $h$th BRB subsystem. $S$ is the total number of the training samples, $\hat{\beta}_{hj} = (\hat{\beta}_{hj}(1), \ldots, \hat{\beta}_{hj}(S))$ represents the observed belief degree of the $j$th consequent state and $\beta_{hj} = (\beta_{hj}(1), \ldots, \beta_{hj}(S))$ is the predicted belief degree of the $j$th consequent state that is generated by the BRB model. The number of parameters in $P_h$ is related to the numbers of belief rules, antecedent attributes, and consequent states, which equals to $(N_h \times L_h + L_h + M_h)$.

### *F. Final Diagnostic Result Generation*

The belief degree of the abnormal state of the $h$th fault mode can be acquired with (1)–(5) which is $\beta_{h2}(h = 1, 2, \ldots, t)$. As described in Section II-A, $p_h = \beta_{h2}(h = 1, 2, \ldots, t)$ and $p_h(h = 1, 2, \ldots, t)$ is used to constitute the final diagnostic result $\{p_1, p_2, \ldots, p_h \ldots, p_n\}$. 0.5 is used as the threshold to evaluate whether the fault mode is positive (the fault occurs) or not. If $p_h(h = 1, 2, \ldots, t)$ exceeds 0.5, the fault mode will be considered to occur; if the belief degrees of the abnormal state of several fault modes are over 0.5, all the corresponding fault modes will be considered to be happened; if no $p_h(h = 1, 2, \ldots, t)$ is above 0.5, the marine diesel engine is considered to be good without any fault.

## III. Application to the Abnormal Wear Detection of Marine Diesel Engines

### *A. Problem Description and Dataset*

A marine diesel engine contains a variety of wear components. Statistics shows that over 50% of faults in marine diesel engines are caused by friction and wear [34]. Detecting abnormal wear timely and accurately is an important aspect of avoiding severe wear faults in marine diesel engines. Among the methods used for wear fault diagnosis of marine diesel engine, spectral analysis is a proven technique to find out abnormal wear positions by analyzing elements' concentrations in lubricating oil since different wear components in a marine diesel engine are made of different materials [35].

For abnormal wear detection in a marine diesel engine, the states (normal and abnormal) of the various wear components and working medium of the engine, such as lubricating oil are considered as fault modes. These fault modes are reflected by the concentration levels of elements in lubricating oil which are considered as fault features. The elements in lubricating oil can be from multiple sources and the abnormal state of one component may make another component become abnormal. For example, once the lubricating oil is polluted by outside contaminants, main bearing may be in abnormal wear subsequently after working in the environment of the polluted lubricating oil. In this application, lubricating oil and three wear components which are main bearing, piston, and cylinder liner-piston ring are considered for wear detection. The materials of the major wear components are listed in Table I [36]. Cylinder liner and piston ring constitutes a friction pair so they are treated as one wear component in this paper. Similarly, since main bearing, bearing bush and bearing journal fit together, they are considered as a whole part.

TABLE I
Material of Wear Components in a Four-Stroke Marine Diesel Engine

| Wear Component | Material | Main Elements |
|---|---|---|
| Cylinder liner | HT 25~47 | Fe, Si |
| Piston ring | Alloy cast iron | Fe, Si |
| Main bearing [a] | ZQPb30, S45C | Cu, Pb, Fe |
| Piston | ZL108 | Al |

[a] Main bearing, bearing bush and bearing journal are considered together.

The concentrations of the elements in lubricating oil can be acquired by analyzing lubricating oil samples with spectral analysis. In this paper, historical samples are collected during the operation of several marine diesel engines which are of the same type and the dataset is expanded to 152 samples based on the mega-trend-diffusion method [37], [38] to keep the numbers of the samples on different wear faults balanced. Every sample contains the concentration of elements Fe, Al, Pb, and Si. There are five kinds of wear faults in the dataset, including abnormal wear of piston, abnormal wear of cylinder liner-piston ring, abnormal wear of main bearing, polluted lubricating oil, and the concurrence of polluted lubricating oil and main bearing wear. Besides the five kinds of wear faults, the samples on normal state are also contained in the dataset. Fig. 4 shows the concentrations of Fe, Al, Pb, and Si, respectively. To test the BRB expert system constructed in the following sections, fivefold cross-validation method is used. The whole dataset is divided into five subsets with similar size. Any four subsets are used as a training dataset with 120 or 122 samples and the fifth subset is used as a testing dataset with 30 or 32 samples. During the training process, the training step of each BRB subsystem is done using the whole training data, considering the patterns from the single class as positive and all other samples are negative. For example, when the training dataset is used to train the BRB subsystem for piston wear, only the samples on abnormal wear of piston are positive (i.e., abnormal wear in piston) and the rest of the samples in the training dataset are considered to be negative (i.e., normal wear in piston).

### *B. BRB Expert System for Abnormal Wear Detection of Marine Diesel Engines*

The BRB expert system contains four BRB subsystems to identify the abnormal wear state of piston, cylinder liner-piston

ring, main bearing, and lubricating oil, respectively. The elements concentrations in lubricating oil are used as antecedent attributes which will be allocated to each BRB subsystem correspondingly. Due to the many-to-many relationship between the element concentrations and the abnormal wear parts, there will be intersection among the antecedent attributes of the four BRB subsystems. As a binary classification model, the outputs of each BRB subsystem include normal state and abnormal state, which is $\Theta = \{state1 = normal; state2 = abnormal\}$. When ignorance exists in a belief rule, $\{normal, abnormal\}$ will be considered as the third consequent state. The final output given by the BRB expert system is in the form {(Piston: $p_1$), (Cylinder liner-piston ring: $p_2$), (Bearing: $p_3$), (lubricating oil: $p_4$)}, where $p_1$, $p_2$, $p_3$, and $p_4$ represents the predicted belief degree of abnormal wear state in each part.

To represent the expert knowledge in abnormal wear detection, referential points for each antecedent attribute are given. Two referential points low (L) and high (H) are essential which equal to the minimum and maximum values of each element's concentration [23]. Consequently, the points between L and H can cover the whole value range of each antecedent attribute.

However, the data ranges of some element concentrations tend to be large from normal state to abnormal state. For example, the minimum concentration of Si is only 1.6 ppm but the maximum concentration is 52.26 ppm. To make the samples represented by belief distributions better distinguish from each other, a referential point middle (M) is added which is a cut-point $c$ of each element concentration range. The samples of which element concentrations on one side of the cut-point $c$ are labeled as abnormal wear and those with values on the other side are labeled as normal wear. The accuracy of such a classification can be determined by the *sensitivity* and *specificity*, where *sensitivity* and *specificity* are the probability of truly identifying abnormal and normal samples at a certain cut-point, respectively. Receiver operating characteristic (ROC) curve is used to determine optimal cut-point, which is a plot of sensitivity versus (1-*specificity*) at all possible cut-points [39], [40]. The optimal cut-point is generally located in the top left part of the ROC curve with the maximum value (*sensitivity* + *specificity* − 1) known as Youden index [41] and it is used as the value of the referential point M. Take the concentration of Al for example. The minimum value (2.9 ppm) and maximum value (26.4 ppm) of Al concentration are selected as referential points L and H, respectively. Since Al is the dominant element indicating abnormal wear of piston, the samples on piston wear are labeled as 1, whereas the other samples are labeled as 0. By using statistical product and service solutions (SPSS), the ROC curve of Al can be acquired as well as coordinate points ($x$-coordinate: sensitivity; $y$- coordinate: 1-specificity) of the curve. It can be found that when 13.35 ppm is used as the cut-point, the corresponding coordinate point is ($x$-coordinate: 1; $y$-coordinate: 0), and (sensitivity + specificity − 1) of this coordinate point equals to 1 which is maximum among the (*sensitivity* + *specificity* − 1) values of all coordinate points. Therefore, 13.35 ppm is selected as the referential point M of Al. The referential point M of other elements can be determined in the same way. The values of the referential points for each antecedent attribute are listed in Table II.

TABLE II
VALUES OF REFERENTIAL POINTS FOR EACH ANTECEDENT ATTRIBUTE (PPM)

| | Fe | Al | Pb | Si |
|---|---|---|---|---|
| Low(L) | 12.50 | 2.90 | 1.95 | 1.60 |
| Middle(M) | 36.95 | 13.35 | 9.63 | 8.07 |
| High(H) | 85.30 | 26.40 | 18.50 | 52.26 |

Each antecedent attribute will be divided by either two (L and H) or three (L, M, H) referential points to construct the rule base of the BRB expert system. The tradeoff between model accuracy and model complexity is taken into account when the number of reference points are selected. The submodel with best accuracy, stability, and validity will be selected finally. Specifically, accuracy is the closeness between the predicted belief degrees and the observed belief degrees of consequent states in a BRB model. Stability describes how the parameters of a BRB model vary with its inputs. Validity indicates whether there is any rule being in conflict with other rules or experts' experience.

### C. BRB Subsystem for Piston

The material of the piston is ZL108, of which the main element is Al as shown in Table I. Consequently, the concentration of Al is selected as the single antecedent attribute in the BRB subsystem for the piston. The BRB subsystems with two referential points and three referential points for Al concentration are constructed, respectively, for comparison. By comparing the accuracy and complexity of the two BRB subsystems with each other, it can be found that the BRB subsystem with two referential points for the concentration of Al can generate more accurate prediction. Therefore, only two rules are included in the BRB subsystem for the abnormal wear detection of the piston. The referential points for the concentration levels of Al are L (L = 2.90 ppm) and H (H = 26.40 ppm). According to (1), the inputs of the BRB subsystem will be transformed into belief distributions. For example, the concentration of Al in one sample is 17.6 ppm, and it will be transformed into {(L:0.376); (H:0.624)} so that $0.376 \times 2.9 + 0.624 \times 26.4 = 17.6$. Then the inference will be conducted based on (2)–(5) to generate the outputs of the model. Using the training dataset described in Section III-A, seven parameters (six of them are shown in Table III and the seventh is the antecedent weight which is 1) of the BRB subsystem for piston are trained. The optimized BRB subsystem which is trained by the first training dataset is listed as Table III and the parameters of the other four BRB subsystems in the fivefold cross-validation can be found in Appendix A1.

### D. BRB Subsystem for Cylinder Liner-Piston Ring

Fe and Si are selected as the antecedent attributes of the BRB system for cylinder liner-piston ring since Fe is the main element of the material of the cylinder liner-piston ring,

TABLE III
BRB SUBSYSTEM FOR PISTON AFTER OPTIMIZATION

| Rule NO. | Rule Weight | Element Concentration in Lubricating Oil | Consequent Distribution | |
|---|---|---|---|---|
| | | Al | Normal | Abnormal |
| 1 | 1 | L | 1 | 0 |
| 2 | 0.938 | H | 0 | 1 |

and cylinder liner-piston ring wear can also produce some Si. However, Fe does not only come from cylinder liner-piston ring wear, but also come from the main bearing wear. Due to the multisources of Fe, it is difficult to identify the wear state of the cylinder liner-piston ring when the antecedent attributes of a rule are in the combination {Fe: H, Si: L}. The samples with {Fe: H, Si: L} can be on the abnormal wear state of the cylinder liner-piston ring or that of the main bearing. To solve the problem, Pb, which is the dominant element for abnormal wear detection of the main bearing, is also used as the antecedent attribute of the BRB subsystem for the cylinder liner-piston ring. By adding Pb into the antecedent attributes, the rule with the antecedent attributes {Fe: H, Si: L} is further divided into two rules

$R_1$: IF: *Fe* is $H \wedge$ *Si* is $L \wedge$ *Pb* is $L$
THEN: wear state of cylinder liner-piston ring is

$$\left\{\left(normal, \beta_1^1\right), \left(abnormal, \beta_2^1\right)\right\}, \left(\sum_{n=1}^{2} \beta_n^1 \leq 1\right).$$

$R_2$: IF: *Fe* is $H \wedge$ *Si* is $L \wedge$ *Pb* is $H$
THEN: wear state of cylinder liner-piston ring is

$$\left\{\left(normal, \beta_1^2\right), \left(abnormal, \beta_2^2\right)\right\}, \left(\sum_{n=1}^{2} \beta_n^2 \leq 1\right)$$

where $\beta_1^1$ is far smaller than $\beta_2^1$ in $R_1$, whereas $\beta_1^2$ is far higher than $\beta_2^2$ in $R_2$.

The numbers of referential points for the concentration levels of Fe, Si, and Pb can be 2 or 3. We have tested and compared all combinations of different numbers of referential points and found that the BRB subsystem in which the numbers of the referential points for all antecedent attributes are 3 performs best in terms of accuracy, stability, and validity which are defined in Section III-B. By traversing the referential points of the antecedent attributes Fe, Si, and Pb, 27 rules are constructed.

Ignorance should be taken into account in the consequent states when Fe, Si, and Pb are all in H level. This is because several totally different combinations of the wear faults can lead to high concentrations of the three elements and the ignorance cannot be eliminated with the information acquired currently. In this occasion, the belief distribution of the output is $\{(normal, 0), (abnormal, 0), ((normal, abnormal), 1)\}$, indicating the complete ignorance in the rule.

One hundred and eleven parameters of the BRB subsystem are optimized by the training dataset according to (6) and the constrains illustrated in (6a)–(6d). The BRB subsystem trained by the first training dataset is shown in Table IV and the parameters of the other four BRB subsystems in the five-fold cross-validation are listed in Appendix A3. In Table IV, the rule weights of the 13th and 14th rules are close to 0, indicating that the two rules hardly play any roles in the abnormal wear detection for cylinder liner-piston ring. In addition, when the concentration level of Fe is L or M, the cylinder liner-piston ring tends to be in normal state. With the concentration level of Fe increasing from L to M, the belief degree of normal state decreases correspondingly, even though the change is slight. On the contrary, there is a high probability for the cylinder liner-piston ring to be in abnormal state when the concentration level of Fe is H except the rule that the concentration level of Pb is also H. Similar trends can also be observed in the other four sub-BRB models trained by the other four training datasets, respectively.

### *E. BRB Subsystem for Main Bearing*

Pb is used as the antecedent attribute of the BRB subsystem for main bearing. By comparing the performance of the BRB subsystem with two referential points for the concentration levels of Pb with that of the BRB subsystem with three referential points, it is proved that the BRB subsystem with three referential points is more appropriate.

After optimization, the BRB subsystem can better describe the relationship between the concentration of Pb and the wear states of the main bearing. The belief rule base for abnormal wear detection of the main bearing after being trained by the first training dataset is shown in Table V. The parameters of the BRB subsystems trained by the other four training datasets can be referred to Appendix A2.

### *F. BRB Subsystem for Lubricating Oil*

Generally external pollutants, such as silt and dust can get into the lubricating oil during the operation of ships and contaminate the oil. Meanwhile, the contaminants can deposit in the mechanical components of the marine diesel engine, exacerbating the abnormal wear of these components. Some wear components are sensitive to the pollution of the lubricating oil, such as the main bearing.

Si is the main element of the silt and dust which is used as the antecedent attribute of the BRB subsystem for lubricating oil. As mentioned above, the external contaminant is not the single source of Si, and the abnormal wear of the piston and the cylinder liner-piston ring can also produce a certain amount of Si. Therefore, when the concentration of Si is in the high level, the ignorance of the state of the lubricating oil will exist. To eliminate the ignorance, the concentrations of Fe and Al are

TABLE IV
BRB SUBSYSTEM FOR CYLINDER LINER-PISTON RING AFTER OPTIMIZATION

| Rule NO. | Rule Weight | Element Concentration in Lubricating Oil | | | Consequent Distribution | | |
|---|---|---|---|---|---|---|---|
| | | Fe | Si | Pb | Normal | Abnormal | {Normal, Abnormal} |
| 1 | 1 | L | L | L | 1 | 0 | 0 |
| 2 | 1 | L | L | M | 1 | 0 | 0 |
| 3 | 1 | L | L | H | 1 | 0 | 0 |
| 4 | 1 | L | M | L | 0.998 | 0 | 0.002 |
| 5 | 1 | L | M | M | 0.998 | 0 | 0.002 |
| 6 | 0.998 | L | M | H | 1 | 0 | 0 |
| 7 | 0.997 | L | H | L | 1 | 0 | 0 |
| 8 | 1 | L | H | M | 1 | 0 | 0 |
| 9 | 1 | L | H | H | 0.998 | 0.001 | 0.001 |
| 10 | 0.996 | M | L | L | 1 | 0 | 0 |
| 11 | 1 | M | L | M | 1 | 0 | 0 |
| 12 | 1 | M | L | H | 1 | 0 | 0 |
| 13 | 0.026 | M | M | L | 0.017 | 0.836 | 0.146 |
| 14 | 0.001 | M | M | M | 0.628 | 0.18 | 0.192 |
| 15 | 1 | M | M | H | 1 | 0 | 0 |
| 16 | 0.953 | M | H | L | 0.958 | 0.038 | 0.004 |
| 17 | 0.986 | M | H | M | 0.98 | 0.02 | 0 |
| 18 | 0.999 | M | H | H | 0.995 | 0.002 | 0.003 |
| 19 | 0.929 | H | L | L | 0.044 | 0.954 | 0.002 |
| 20 | 0.587 | H | L | M | 0.358 | 0.456 | 0.185 |
| 21 | 1 | H | L | H | 1 | 0 | 0 |
| 22 | 1 | H | M | L | 0 | 1 | 0 |
| 23 | 0.657 | H | M | M | 0.154 | 0.846 | 0 |
| 24 | 1 | H | M | H | 1 | 0 | 0 |
| 25 | 0.999 | H | H | L | 0 | 0.999 | 0.001 |
| 26 | 0.999 | H | H | M | 0 | 0.715 | 0.285 |
| 27 | 1 | H | H | H | 0 | 0 | 1 |

TABLE V
BRB SUBSYSTEM FOR MAIN BEARING AFTER OPTIMIZATION

| Rule NO. | Rule Weight | Element Concentration in Lubricating Oil | Consequent Distribution | |
|---|---|---|---|---|
| | | Pb | Normal | Abnormal |
| 1 | 1 | L | 1 | 0 |
| 2 | 0.001 | M | 0.347 | 0.653 |
| 3 | 1 | H | 0 | 1 |

also used as the antecedent attributes of the BRB subsystem for the polluted lubricating oil.

By comparing the BRB subsystems for the detection of polluted lubricating oil with different numbers of referential points for each antecedent attributes, it can be found that the BRB subsystem containing 12 rules can achieve a better tradeoff between the model accuracy and complexity. In this subsystem, the numbers of referential points are 3 (L, M, H), 2 (L, H), and 2 (L, H) for the concentration levels of Si, Fe, and Al, respectively. The complete ignorance is also considered in the consequent attribute besides the normal state and the abnormal state when all the concentrations of the three elements are in high level. Table VI gives the optimized belief rule base which is trained by the first training dataset. The parameters of the BRB subsystems trained by the other four training datasets are listed in Appendix A4. In Table VI, it can be found the state of lubricating oil will be normal as long as the concentration level of Si is L, but the concentration levels of Fe and Al have an effect on the state of lubricating oil when the concentration level of Si is M or H. Specifically, as indicated by the fifth and ninth rules, the lubricating oil has an extremely high probability of being abnormal when the concentration levels of Fe and Al are both L, and the higher the concentration level of Si, the more important the corresponding rule in the rule base (0.235 for the fifth rule and 0.997 for the ninth rule). However, when the concentration level of Si is M, there will be a high probability of lubricating oil being in normal state as long as one of Fe and Al is in H concentration level. Due to the limitation of our current knowledge, high belief degree will be assigned to ignorance when the concentration levels of Si and either Fe or Al are H. Moreover, the multiple sources of Fe reduces the credibility of the seventh rule, making this rule hardly have any effect on the final result with a rule weight 0.001. Similar trends can also be observed in the other four sub-BRB models trained by the other four training datasets.

TABLE VI
BRB SUBSYSTEM FOR LUBRICATING OIL AFTER OPTIMIZATION

| Rule NO. | Rule Weight | Element Concentration in Lubricating Oil | | | Consequent Distribution | | |
|---|---|---|---|---|---|---|---|
| | | Si | Fe | Al | Normal | Abnormal | {Normal, Abnormal} |
| 1 | 1 | L | L | L | 1 | 0 | 0 |
| 2 | 1 | L | L | H | 1 | 0 | 0 |
| 3 | 1 | L | H | L | 1 | 0 | 0 |
| 4 | 1 | L | H | H | 1 | 0 | 0 |
| 5 | 0.235 | M | L | L | 0 | 1 | 0 |
| 6 | 0.997 | M | L | H | 1 | 0 | 0 |
| 7 | 0.001 | M | H | L | 0.998 | 0.002 | 0 |
| 8 | 1 | M | H | H | 1 | 0 | 0 |
| 9 | 0.997 | H | L | L | 0 | 1 | 0 |
| 10 | 0.924 | H | L | H | 0.011 | 0.002 | 0.987 |
| 11 | 0.686 | H | H | L | 0.005 | 0.128 | 0.867 |
| 12 | 0.973 | H | H | H | 0.009 | 0 | 0.991 |

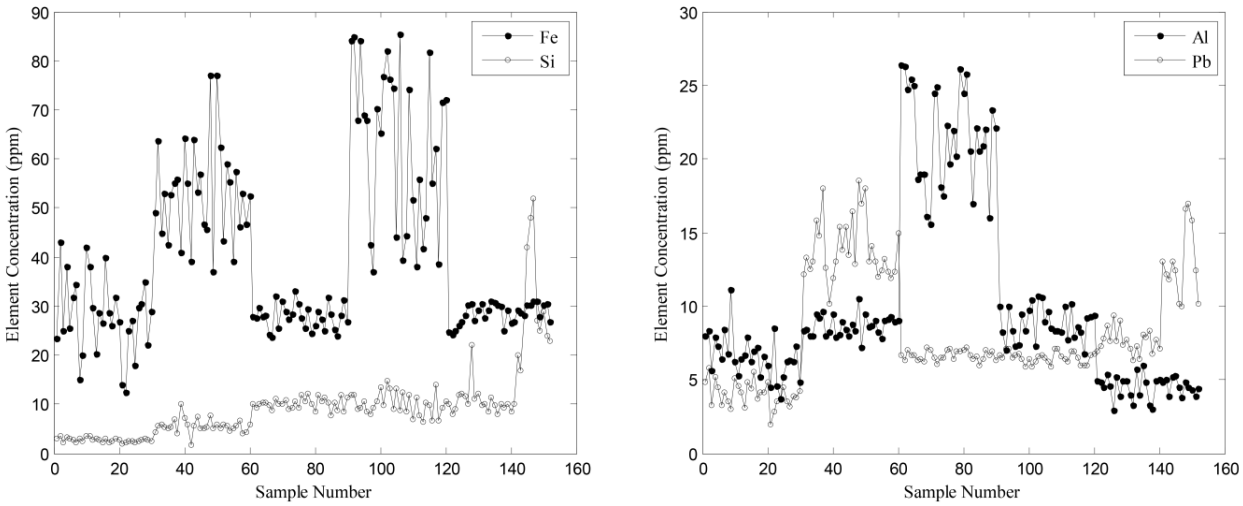


Fig. 4. Concentrations of elements Fe, Si, Al, and Pb in the dataset (a) concentration of Fe and Si and (b) concentration of Al and Pb.

## IV. VALIDATION OF THE BRB EXPERT SYSTEM

Abnormal wear detection of marine diesel engines is still used as the example to verify the effectiveness of the BRB expert system for fault diagnosis.

As described previously, fivefold cross-validation is conducted to evaluate the robustness of the BRB expert system. To further verify the performance of the optimized BRB expert system, the results of the abnormal wear detection given by the optimized BRB expert system are compared with those given by ANN models, SVM models, and the initial BRB expert system which can be treated as a model based on expert experiences only. We constructed two ANN models and two SVM models with different structures. The first ANN model and the first SVM model share the similar structure with the BRB expert system, containing four subsystems for detecting abnormal states of piston, cylinder liner-piston ring, main bearing, and lubricating oil, respectively. In the second ANN model and the second SVM model, the concentration levels of elements Fe, Al, Pb, and Si are used as the inputs and six modes (including five fault modes and the normal mode) contained in the training dataset are used as the outputs. Therefore, there are four nodes in the input layer and six nodes in the output layer in the second ANN model, and four inputs and six outputs in the second SVM model. To demonstrate the overall performance of the models mentioned above, we use user accuracy (UA) [42] to show the result. UA is the ratio of the number of correctly detected samples to the number of samples on this component. Fig. 5 shows the UA variation of testing datasets given by the six different models in fivefold cross-validation. In Fig. 5, onefold in the horizontal axis represents the model is trained by the first training dataset and so on. The vertical axis represents the values of UA.

From Fig. 5, it can be seen that the optimized BRB expert system has the best performance on abnormal wear detection. All the UA values are above 80% in the fivefold cross-validation test. Especially in the secondfold and fourth fold tests, all the samples in the testing datasets are identified correctly. Moreover, the optimized BRB expert system is more stable than other models and there is not an obvious fluctuation of UAs in the fivefold cross-validation test. The ANN model

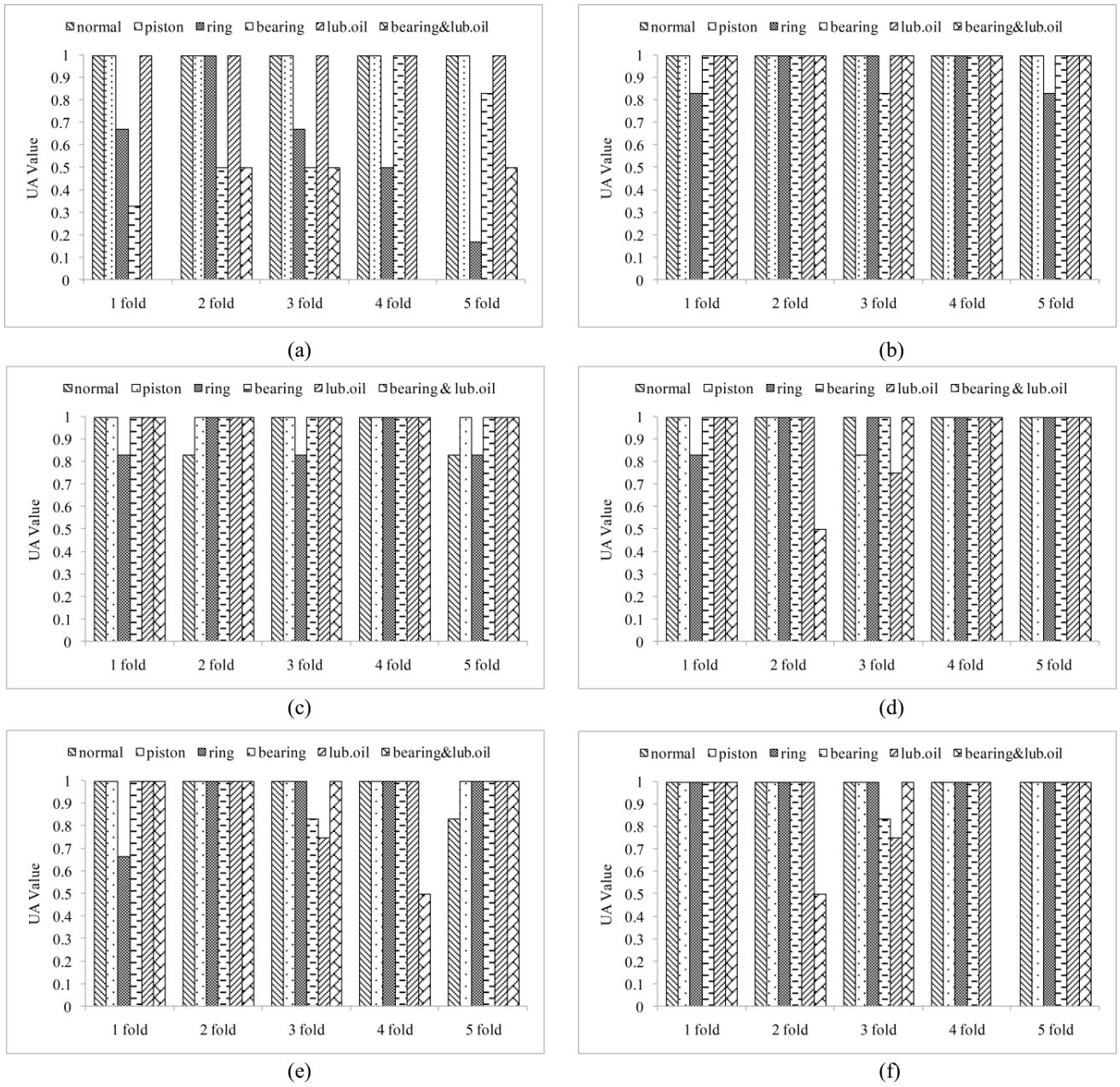


Fig. 5. UA of the testing datasets in fivefold cross-validation given by (a) initial BRB expert system, (b) optimized BRB expert system, (c) ANN model with four ANN subsystems, (d) ANN model with six outputs, (e) SVM model with four SVM subsystems, and (f) SVM models with six outputs.

containing four ANN subsystems has a similar performance both in accuracy and stability, but in the second and fifth fold tests the performance of the ANN group model on the identification of normal samples is not as good as that of the optimized BRB expert system. The ANN model with six outputs and the SVM model with four SVM subsystems have the moderate performance either on accuracy or on stability. Although the SVM model with six outputs performs best on detecting abnormal wear of cylinder liner-piston ring, it cannot identify the concurrent faults stably, especially in the fourth round. The initial BRB expert system which is only based on expert experience performs worse than the other models. Specifically, with the initial BRB expert system, some UAs of detecting cylinder liner-piston ring and concurrent faults are below 50%, and the UAs of detecting cylinder liner-piston ring and main bearing using the initial BRB expert system fluctuate significantly.

Although the ANN group model has a similar performance to the optimized BRB expert system, its identification accuracy is influenced by the number of hidden layer nodes. Based on the empirical equation $n_h = \sqrt{n+m} + a$ [43], where $n$ is the number of input layer nodes, $m$ the number of output layer nodes, $a$ an integer between 0 and 10, and $n_h$ the number of hidden layer nodes in the ANN models. In each fold, $a$ varies from 0 to 10 and the number of hidden layer nodes which makes the ANN model perform better with the training

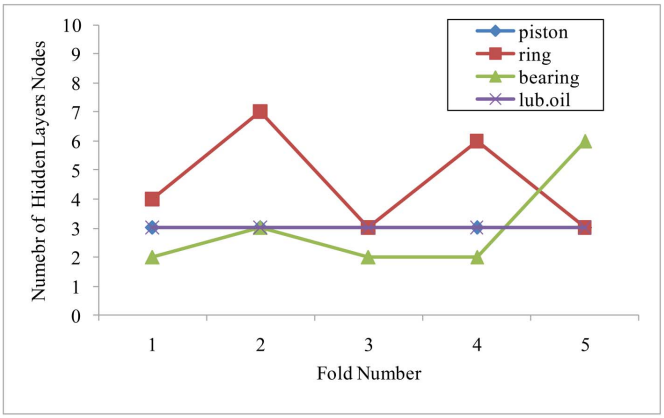


Fig. 6. Number of hidden layer nodes in fivefold cross-validation test for the ANN model with four ANN subsystems.

dataset is selected. Fig. 6 shows the variation of the number of hidden layer nodes in the fivefold cross-validation test.

From Fig. 6, it can be seen that the numbers of the hidden layers nodes in the ANN subsystems for piston and lubricating oil are stable which are all 3. But the numbers of the hidden layers nodes in the sub-ANN models for cylinder liner-piston ring and main bearing vary obviously with different training datasets which change between 3 to 7 and between 2 to 6, respectively. Compared with the ANN models, the structure of the BRB expert system does not change from fold to fold after optimization, with only slight changes in parameters as shown in Appendix A. This indicates the robustness and credibility of the BRB expert system.

Besides ANN models, a binary logistic regression model which is used to estimate the probability of a binary response to one or several independent variables is also applied to construct an abnormal wear detection model for marine diesel engine using SPSS. Similar to the BRB expert system, ANN model with four subsystems, and SVM model with four subsystems, the whole model is also divided into four submodels for each component and each submodel is constructed by binary logistic regression. However, as the number of samples on abnormal wear of different wear components from real ships is limited, the samples tend to be distributed at either normal or abnormal end and there are not enough samples in the transition phase from normal to abnormal, the feasibility of the abnormal wear detection model based on binary logistic regression cannot be ensured. For example, in the abnormal wear detection model for piston, the concentration of Al is used as the independent variable and the wear state ($normal = 0$ and $abnormal = 1$) is used as the categorical dependent variable. A logistic regression function can be acquired to represent the relationship between the concentration of Al and the wear state of piston, but the relationship between the concentration of Al and the wear state of piston is insignificantly correlated with each other at $p<0.05$ level, indicating that the concentration of Al is not significantly associated with the probability of the piston being in abnormal state. This result contradicts with the knowledge that the concentration of Al is the main feature indicating the wear state of piston as we described previously. This is because there are no samples between the maximum concentration of Al in normal range (11.1 ppm) and minimum concentration of Al in abnormal range (15.6 ppm), causing uncertainty in the parameters of the logistic regression. As a result, the significant role of Al concentration cannot be recognized and reflected in the final regression function.

Based on the discussion about the performance of the BRB expert system in fivefold cross-validation, a model which is suitable for detecting various types of abnormal wear of engines is determined. As Fig. 5(b) indicated, the BRB expert system trained by the second and fourth training datasets can both perform well on the testing datasets. Considering the performance of the BRB expert system on the whole dataset, the system constructed using the fourth training dataset is used as the final BRB model.

Fig. 7 shows the predicted belief degrees of abnormal state in the fourth testing dataset. The belief degrees in Fig. 7(a) and (b) are given by the initial BRB expert system and the BRB expert system trained by the fourth training dataset. In Fig. 7, each sample corresponds to four predicted belief degrees which represent the belief degrees of abnormal state of piston (P), bearing (B), cylinder liner-piston ring (R), and lubricating oil (L), respectively. For example, the four values of the 19th sample in Fig. 7(a) are $\{p_1 = 0.181, p_2 = 0.895, p_3 = 0.015, p_4 = 0.047\}$, which indicates that the probabilities of the 19th sample being in abnormal state of piston, cylinder liner-piston ring, main bearing, and lubricating oil are 0.181, 0.895, 0.015, and 0.047, respectively. Since only the belief degree of abnormal state of cylinder liner-piston ring exceeds the threshold 0.5, this sample indicates that the cylinder liner-piston ring is in abnormal wear state.

As described in Section III, ignorance is considered in the BRB subsystems for cylinder liner-piston ring and lubricating oil. The ignorance (the belief degree associated with an unknown state in a prediction) of sample 19, 20, and 22 on abnormal wear of cylinder liner-piston ring marked by the rectangle in Fig. 7(a) is obvious. For the three samples, the belief degrees of abnormal state of cylinder liner-piston ring are 0.801, 0.775, and 0.922, with the ignorance 0.097, 0.097, and 0.093 correspondingly. After optimization, the ignorance of these samples is small enough to be ignored. The belief degrees of abnormal state of cylinder liner-piston ring are 0.895, 0.935, and 0.95, respectively. Meanwhile, the ignorance of the samples on polluted lubricating oil is small no matter whether the predication is given by the initial BRB expert system or by the BRB expert system after optimization. The falsely identified samples in the testing dataset are marked by black ovals. By comparing Fig. 7(a) and (b), it can be found the optimized BRB expert system reduces the number of falsely identified samples from five to zero. Moreover, the optimized BRB expert system makes the distinction between the normal wear state and abnormal wear state clearer by giving a higher belief degree to abnormal state of the abnormal components and a lower belief degree to abnormal state of the normal components.

As shown in Fig. 6, the number of hidden layer nodes of each ANN subsystem varies in the fivefold cross-validation causing changes to the structures of the ANN model with

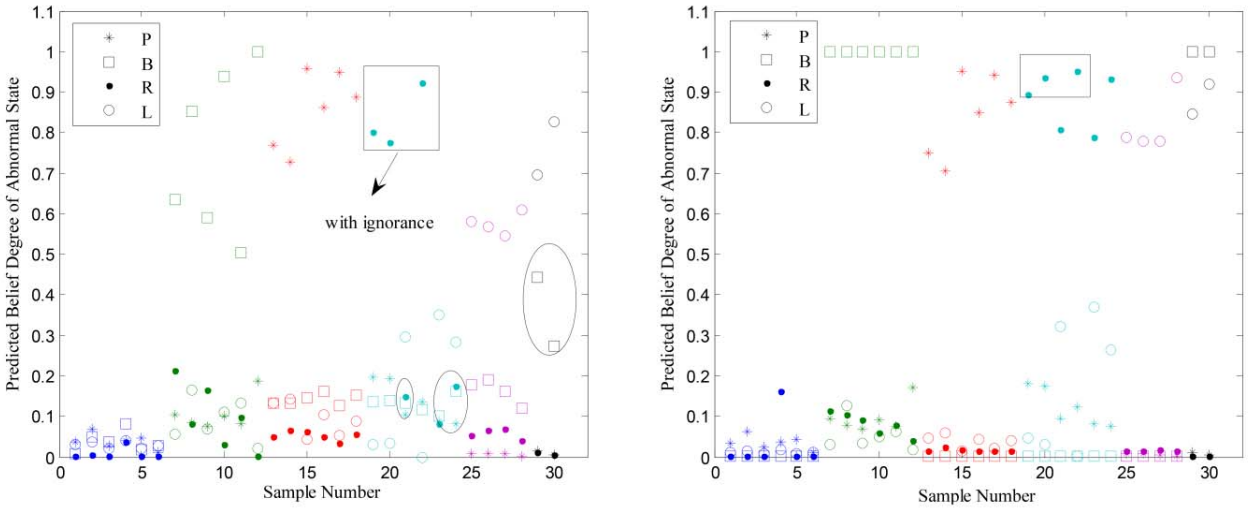


Fig. 7. Predicted belief degrees of abnormal state in the fourth testing dataset given by (a) initial BRB expert system, (b) optimized BRB expert system (P: piston; B: main bearing; R: cylinder liner-piston ring; L: lubricating oil).

four subsystems in every fold. To determine a model which can perform well in every test, the performances of the ANN models in 12 possible structures are compared. The UAs of the testing datasets in fivefold cross-validation given by the 12 possible ANN group models are shown in Fig. 8. From this figure, it can be found that the ANN group model with 3, 3, 6, and 3 hidden layer nodes in the ANN subsystems for piston, cylinder liner-piston ring, main bearing, and lubricating oil performs best no matter in accuracy or in stability. It can also be found that the ANN models with different structures have different performances in the fivefold cross-validation, which further indicates that the structure of ANN model is not robust.

## V. Application Example of the BRB Expert System on Abnormal Wear Detection

In this section, the samples from the 1000-h reliability test of a four-stroke diesel engine are used to illustrate the inference process of the BRB expert system constructed in Section III. The materials of the components of the engine are very similar to those from which the samples used in Sections III and IV were collected. The 1000-h reliability test was conducted. During the experiment, the lubricating oil was sampled every 48 h and the spectral data was acquired by spectral analysis. We use the optimized BRB expert system to detect the wear state of the marine diesel engine with the sample collected at the 912th h. The concentrations of the particles in this sample is listed as follows:

Sample at the 912th h: {(Fe: 92.5 ppm), (Al: 8.8 ppm), (Pb: 10.7 ppm), (Si: 7.7 ppm)}.

The subinputs to the BRB subsystems for piston, cylinder liner-piston ring, main bearing, and lubricating oil are {Al}, {Fe, Si, Pb}, {Pb}, and {Fe, Al, Si} correspondingly. Using (1) and the values of the referential points in Table II, the concentrations of the elements are transformed into belief distributions over the referential values, which are as follows.

In the BRB subsystem for piston: {Al: (L: 0.749); (H: 0.251)}.

In the BRB subsystem for cylinder liner-piston ring: {Fe: (L: 0); (M: 0); (H: 1)}; {Si: (L: 0.057); (M: 0.943); (H: 0)}; {Pb: (L: 0); (M: 0.879); (H: 0.121)}.

In the BRB subsystem for main bearing: {Pb: (L: 0); (M: 0.879); (H: 0.121)}.

In the BRB subsystem for lubricating oil: {Fe: (L: 0); (H: 1)}; {Al: (L: 0.749); (H: 0.251)}; {Si: (L: 0.057); (M: 0.943); (H: 0)}.

After the inputs are transformed into belief distribution, the activation weight of each rule in each BRB subsystem can be calculated using (2). For the sample collected at 912th h, the activation weights of each rule in every subsystem are listed as follows.

In the BRB subsystem for piston: $\{\omega_1 = 0.759; \omega_2 = 0.241\}$.

In the BRB subsystem for cylinder liner-piston ring: only the 20th, 21st, 23rd, and 24th rules are activated and the rule activation weights are $\{\omega_{20} = 0.024; \omega_{21} = 0.026; \omega_{23} = 0.482; \omega_{24} = 0.468\}$. The rule activation weights of the other rules are all zero.

In the BRB subsystem for main bearing: $\{\omega_1 = 0; \omega_2 = 0.007; \omega_3 = 0.993\}$.

In the BRB subsystem for lubricating oil: only the 3rd, 4th, 7th, and 8th rules are activated with activation weights $\{\omega_3 = 0.149; \omega_4 = 0.05; \omega_7 = 0.208; \omega_8 = 0.593\}$, and the rule activation weights of the other rules are all zero.

Using the ER approach as described by (3)–(5), we can calculate the belief degrees of the consequent states in each BRB subsystem. The results given by these subsystems are as follows, where $\beta_1$ and $\beta_2$ are belief degrees associated with normal and abnormal states, respectively.

In the BRB subsystem for piston: $\{\beta_1 = 0.91; \beta_2 = 0.09\}$.

In the BRB subsystem for cylinder liner-piston ring: $\{\beta_1 = 0.624; \beta_2 = 0.374; \beta_3 = 0.002\}$.

In the BRB subsystem for main bearing: $\{\beta_1 = 0; \beta_2 = 1\}$.

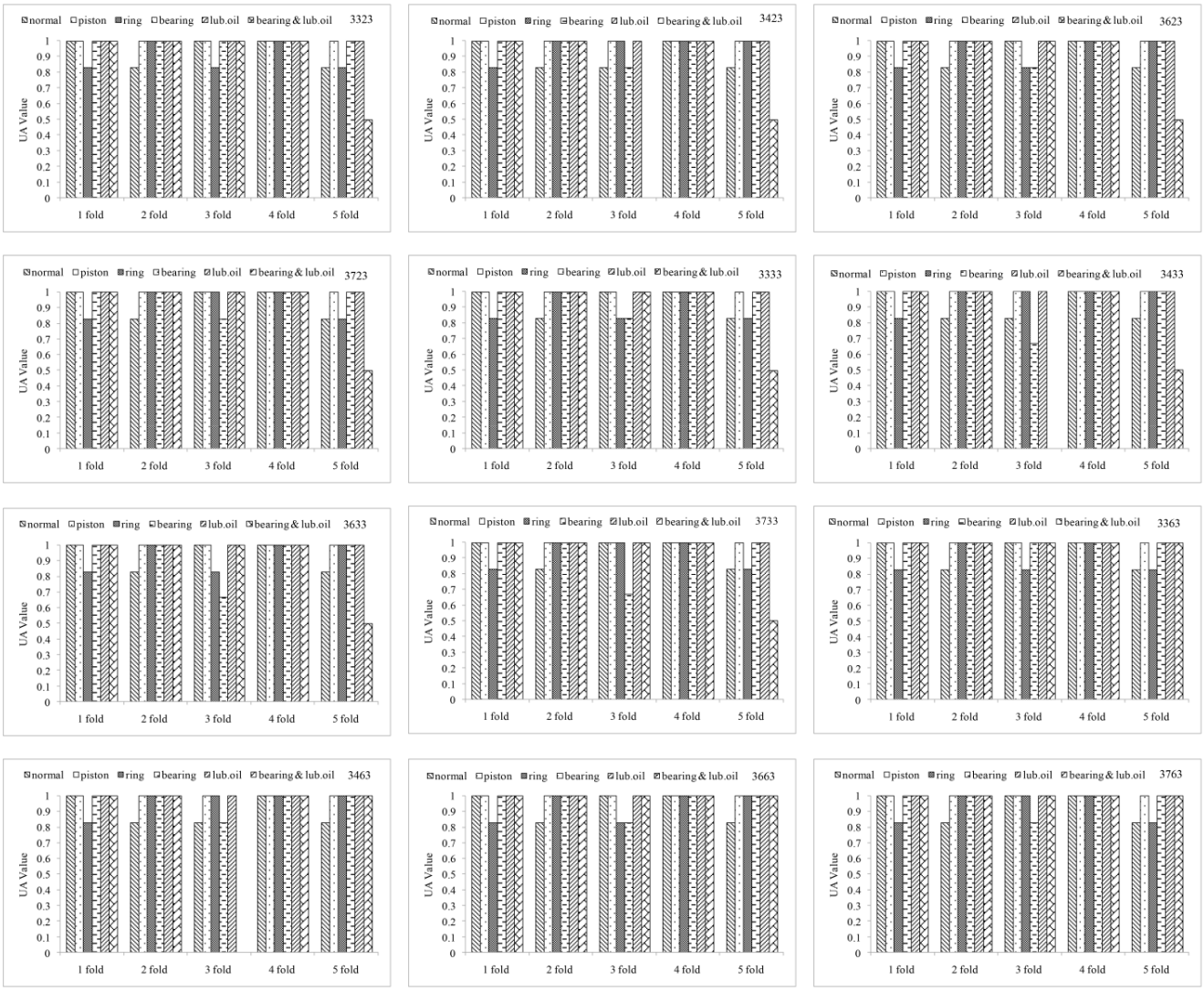


Fig. 8. UA of the testing datasets in fivefold cross-validation given by 12 possible ANN group model structures (e.g., model structure 3323 means there are 3, 3, 2, and 3 hidden layer nodes in the ANN subsystems for piston, cylinder liner-piston ring, main bearing, and lubricating oil, respectively).


Fig. 9. Abnormal wear in the bush of main bearing.

In the BRB subsystem for lubricating oil: $\{\beta_1 = 1; \beta_2 = 0; \beta_3 = 0\}$.

The final result given by the optimized BRB expert system is: $\{p_1 = 0.09; p_2 = 0.374; p_3 = 1; p_4 = 0\}$. The result $p_3 = 1$ indicate that the main bearing is considered to be in abnormal wear state. Moreover, the predicted results from sample collected at 960th h and 1000th h are $\{p_1 = 0.1; p_2 = 0.337; p_3 = 1; p_4 = 0\}$ and $\{p_1 = 0.1; p_2 = 0.290; p_3 = 1; p_4 = 0\}$, which also indicate that the main bearing are in abnormal wear state.

In the overhaul of the diesel engine after 1000-h reliability test, it is found that surface peeling and scorching have occurred in the bottom of the bearing bush of the third main bearing as shown in Fig. 9, which is in agreement with the predicted results of the BRB expert system.

## VI. Conclusion

Effective and timely fault diagnosis is significant to improve the reliability of marine diesel engines. In this paper, we propose a novel fault diagnostic structure and use BRB inference methodology to link the fault modes of marine diesel engines with their fault features. A case study was conducted for the application of the BRB expert system to identifying the abnormal wear in marine diesel engines. With fivefold cross-validation, the effectiveness of the BRB expert system for fault diagnosis of marine diesel engine is compared with that of ANN fault diagnostic model and SVM fault diagnostic model. The major conclusions of this paper are as follows.

$$\delta: \begin{array}{c} \begin{matrix} \text{1st} & \text{2nd} & \text{3rd} & \text{4th} & \text{5th} \end{matrix} \\ \begin{bmatrix} 0.243 & 0.209 & 0.180 & 0.221 & 0.286 \\ 0.557 & 0.613 & 0.510 & 0.655 & 0.535 \\ 0.200 & 0.178 & 0.310 & 0.124 & 0.179 \end{bmatrix} \end{array}$$

$$\begin{array}{cccc} \beta_1 & \beta_2 & \beta_3 & \theta \end{array}$$

$$\begin{bmatrix}
1.000 & 0.000 & 0.000 & 1.000 \\ 1.000 & 0.000 & 0.000 & 1.000 \\ 1.000 & 0.000 & 0.000 & 1.000 \\ 0.998 & 0.000 & 0.002 & 1.000 \\ 0.998 & 0.000 & 0.002 & 1.000 \\ 1.000 & 0.000 & 0.000 & 0.998 \\ 1.000 & 0.000 & 0.000 & 0.997 \\ 1.000 & 0.000 & 0.000 & 1.000 \\ 0.998 & 0.001 & 0.001 & 1.000 \\ 1.000 & 0.000 & 0.000 & 0.996 \\ 1.000 & 0.000 & 0.000 & 1.000 \\ 1.000 & 0.000 & 0.000 & 1.000 \\ 0.017 & 0.836 & 0.146 & 0.026 \\ 0.628 & 0.180 & 0.192 & 0.001 \\ 1.000 & 0.000 & 0.000 & 1.000 \\ 0.958 & 0.038 & 0.004 & 0.953 \\ 0.980 & 0.020 & 0.000 & 0.986 \\ 0.995 & 0.002 & 0.003 & 0.999 \\ 0.044 & 0.954 & 0.002 & 0.929 \\ 0.358 & 0.456 & 0.185 & 0.587 \\ 1.000 & 0.000 & 0.000 & 1.000 \\ 0.000 & 1.000 & 0.000 & 1.000 \\ 0.154 & 0.846 & 0.000 & 0.657 \\ 1.000 & 0.000 & 0.000 & 1.000 \\ 0.000 & 0.999 & 0.001 & 0.999 \\ 0.000 & 0.715 & 0.285 & 0.999 \\ 0.000 & 0.000 & 1.000 & 1.000
\end{bmatrix}
\begin{bmatrix}
1.000 & 0.000 & 0.000 & 1.000 \\ 1.000 & 0.000 & 0.000 & 1.000 \\ 1.000 & 0.000 & 0.000 & 1.000 \\ 1.000 & 0.000 & 0.000 & 1.000 \\ 1.000 & 0.000 & 0.000 & 1.000 \\ 0.999 & 0.001 & 0.000 & 0.999 \\ 1.000 & 0.000 & 0.000 & 1.000 \\ 0.998 & 0.001 & 0.001 & 1.000 \\ 1.000 & 0.000 & 0.000 & 0.999 \\ 0.993 & 0.000 & 0.007 & 0.989 \\ 1.000 & 0.000 & 0.000 & 0.988 \\ 1.000 & 0.000 & 0.000 & 0.991 \\ 0.000 & 0.887 & 0.113 & 0.061 \\ 0.613 & 0.369 & 0.018 & 0.001 \\ 1.000 & 0.000 & 0.000 & 1.000 \\ 0.954 & 0.041 & 0.005 & 0.941 \\ 0.991 & 0.009 & 0.001 & 0.966 \\ 0.998 & 0.001 & 0.001 & 1.000 \\ 0.058 & 0.941 & 0.001 & 0.920 \\ 0.340 & 0.478 & 0.182 & 0.595 \\ 1.000 & 0.000 & 0.000 & 0.988 \\ 0.000 & 1.000 & 0.000 & 1.000 \\ 0.000 & 1.000 & 0.000 & 0.600 \\ 1.000 & 0.000 & 0.000 & 0.980 \\ 0.000 & 1.000 & 0.000 & 1.000 \\ 0.003 & 0.715 & 0.282 & 0.998 \\ 0.000 & 0.000 & 1.000 & 1.000
\end{bmatrix}
\begin{bmatrix}
1.000 & 0.000 & 0.000 & 1.000 \\ 1.000 & 0.000 & 0.000 & 1.000 \\ 1.000 & 0.000 & 0.000 & 1.000 \\ 1.000 & 0.000 & 0.000 & 0.999 \\ 1.000 & 0.000 & 0.000 & 0.999 \\ 1.000 & 0.000 & 0.000 & 1.000 \\ 1.000 & 0.000 & 0.000 & 1.000 \\ 1.000 & 0.000 & 0.000 & 1.000 \\ 1.000 & 0.000 & 0.000 & 1.000 \\ 0.993 & 0.005 & 0.002 & 0.945 \\ 1.000 & 0.000 & 0.000 & 1.000 \\ 1.000 & 0.000 & 0.000 & 1.000 \\ 0.000 & 0.827 & 0.173 & 0.089 \\ 0.343 & 0.618 & 0.038 & 0.001 \\ 1.000 & 0.000 & 0.000 & 1.000 \\ 0.953 & 0.038 & 0.009 & 0.953 \\ 0.993 & 0.007 & 0.000 & 0.952 \\ 1.000 & 0.000 & 0.000 & 1.000 \\ 0.024 & 0.976 & 0.000 & 0.952 \\ 0.365 & 0.472 & 0.164 & 0.547 \\ 0.948 & 0.052 & 0.000 & 0.969 \\ 0.000 & 1.000 & 0.000 & 1.000 \\ 0.000 & 0.987 & 0.013 & 0.748 \\ 1.000 & 0.000 & 0.000 & 1.000 \\ 0.051 & 0.920 & 0.029 & 0.957 \\ 0.120 & 0.653 & 0.227 & 1.000 \\ 0.000 & 0.000 & 1.000 & 1.000
\end{bmatrix}$$

$$\begin{array}{cccc} \beta_1 & \beta_2 & \beta_3 & \theta \end{array}$$

$$\begin{bmatrix}
1.000 & 0.000 & 0.000 & 1.000 \\ 1.000 & 0.000 & 0.000 & 1.000 \\ 1.000 & 0.000 & 0.000 & 1.000 \\ 1.000 & 0.000 & 0.000 & 1.000 \\ 1.000 & 0.000 & 0.000 & 0.999 \\ 1.000 & 0.000 & 0.000 & 1.000 \\ 1.000 & 0.000 & 0.000 & 1.000 \\ 1.000 & 0.000 & 0.000 & 1.000 \\ 0.999 & 0.001 & 0.000 & 1.000 \\ 0.989 & 0.004 & 0.007 & 0.883 \\ 0.999 & 0.000 & 0.001 & 0.981 \\ 1.000 & 0.000 & 0.000 & 1.000 \\ 0.079 & 0.789 & 0.132 & 0.087 \\ 0.734 & 0.257 & 0.009 & 0.001 \\ 1.000 & 0.000 & 0.000 & 1.000 \\ 0.975 & 0.023 & 0.002 & 0.955 \\ 0.998 & 0.002 & 0.000 & 0.985 \\ 0.997 & 0.002 & 0.001 & 1.000 \\ 0.090 & 0.882 & 0.027 & 0.903 \\ 0.343 & 0.473 & 0.184 & 0.575 \\ 1.000 & 0.000 & 0.000 & 0.919 \\ 0.000 & 1.000 & 0.000 & 1.000 \\ 0.190 & 0.810 & 0.000 & 0.707 \\ 1.000 & 0.000 & 0.000 & 1.000 \\ 0.071 & 0.901 & 0.028 & 0.952 \\ 0.151 & 0.637 & 0.212 & 0.999 \\ 0.000 & 0.000 & 1.000 & 1.000
\end{bmatrix}
\begin{bmatrix}
1.000 & 0.000 & 0.000 & 1.000 \\ 1.000 & 0.000 & 0.000 & 1.000 \\ 1.000 & 0.000 & 0.000 & 1.000 \\ 1.000 & 0.000 & 0.000 & 1.000 \\ 1.000 & 0.000 & 0.000 & 1.000 \\ 1.000 & 0.000 & 0.000 & 1.000 \\ 1.000 & 0.000 & 0.000 & 1.000 \\ 1.000 & 0.000 & 0.000 & 1.000 \\ 1.000 & 0.001 & 0.000 & 1.000 \\ 0.993 & 0.005 & 0.002 & 0.946 \\ 1.000 & 0.000 & 0.001 & 0.995 \\ 1.000 & 0.000 & 0.000 & 1.000 \\ 0.000 & 0.869 & 0.131 & 0.186 \\ 0.641 & 0.330 & 0.029 & 0.001 \\ 1.000 & 0.000 & 0.000 & 1.000 \\ 0.935 & 0.062 & 0.002 & 0.920 \\ 0.991 & 0.001 & 0.008 & 0.940 \\ 1.000 & 0.000 & 0.000 & 1.000 \\ 0.001 & 0.999 & 0.000 & 0.994 \\ 0.320 & 0.466 & 0.214 & 0.609 \\ 1.000 & 0.000 & 0.000 & 1.000 \\ 0.000 & 1.000 & 0.000 & 0.984 \\ 0.032 & 0.968 & 0.000 & 0.741 \\ 1.000 & 0.000 & 0.000 & 1.000 \\ 0.004 & 0.995 & 0.001 & 0.999 \\ 0.007 & 0.723 & 0.270 & 0.993 \\ 0.000 & 0.000 & 1.000 & 1.000
\end{bmatrix}$$

With respect to the new structure of the BRB fault diagnostic model, fault diagnosis which is a multiclass classification problem is transformed into several parallel binary classification problems and the model in this structure can identify the concurrent fault modes simultaneously. Since each BRB subsystem has its own antecedent attributes, the complexity of each subsystem can be reduced. During the construction of the BRB expert system for fault diagnosis, some issues

| 1st | 2nd | 3rd | 4th | 5th |
|---|---|---|---|---|
| 0.34 | 0.34 | 0.34 | 0.31 | 0.34 |
| 0.33 | 0.33 | 0.33 | 0.35 | 0.33 |
| 0.33 | 0.33 | 0.33 | 0.34 | 0.33 |

| $\beta_1$ | $\beta_2$ | $\beta_3$ | $\theta$ |
|---|---|---|---|
| 1.000 | 0.000 | 0.000 | 1.000 |
| 1.000 | 0.000 | 0.000 | 1.000 |
| 1.000 | 0.000 | 0.000 | 1.000 |
| 1.000 | 0.000 | 0.000 | 1.000 |
| 0.000 | 1.000 | 0.000 | 0.235 |
| 1.000 | 0.000 | 0.000 | 0.997 |
| 0.998 | 0.002 | 0.000 | 0.001 |
| 1.000 | 0.000 | 0.000 | 1.000 |
| 0.000 | 1.000 | 0.000 | 0.997 |
| 0.011 | 0.002 | 0.987 | 0.924 |
| 0.005 | 0.128 | 0.867 | 0.686 |
| 0.009 | 0.000 | 0.991 | 0.973 |

| $\beta_1$ | $\beta_2$ | $\beta_3$ | $\theta$ |
|---|---|---|---|
| 1.000 | 0.000 | 0.000 | 1.000 |
| 1.000 | 0.000 | 0.000 | 1.000 |
| 1.000 | 0.000 | 0.000 | 1.000 |
| 1.000 | 0.000 | 0.000 | 1.000 |
| 0.000 | 0.987 | 0.013 | 0.203 |
| 1.000 | 0.000 | 0.000 | 1.000 |
| 0.998 | 0.000 | 0.002 | 0.001 |
| 1.000 | 0.000 | 0.000 | 1.000 |
| 0.000 | 0.999 | 0.001 | 0.996 |
| 0.014 | 0.006 | 0.980 | 0.873 |
| 0.004 | 0.252 | 0.744 | 0.418 |
| 0.012 | 0.000 | 0.988 | 0.955 |

| $\beta_1$ | $\beta_2$ | $\beta_3$ | $\theta$ |
|---|---|---|---|
| 1.000 | 0.000 | 0.000 | 1.000 |
| 1.000 | 0.000 | 0.000 | 1.000 |
| 1.000 | 0.000 | 0.000 | 1.000 |
| 1.000 | 0.000 | 0.000 | 1.000 |
| 0.000 | 0.995 | 0.005 | 0.207 |
| 1.000 | 0.000 | 0.000 | 1.000 |
| 1.000 | 0.000 | 0.000 | 0.001 |
| 1.000 | 0.000 | 0.000 | 1.000 |
| 0.000 | 1.000 | 0.001 | 1.000 |
| 0.010 | 0.008 | 0.982 | 0.892 |
| 0.000 | 0.216 | 0.784 | 0.510 |
| 0.008 | 0.000 | 0.992 | 0.966 |

| $\beta_1$ | $\beta_2$ | $\beta_3$ | $\theta$ |
|---|---|---|---|
| 1.000 | 0.000 | 0.000 | 1.000 |
| 1.000 | 0.000 | 0.000 | 1.000 |
| 1.000 | 0.000 | 0.000 | 1.000 |
| 1.000 | 0.000 | 0.000 | 1.000 |
| 0.000 | 0.994 | 0.006 | 0.271 |
| 1.000 | 0.000 | 0.000 | 0.998 |
| 1.000 | 0.000 | 0.000 | 0.118 |
| 1.000 | 0.000 | 0.000 | 1.000 |
| 0.000 | 0.998 | 0.002 | 0.999 |
| 0.005 | 0.007 | 0.988 | 0.921 |
| 0.006 | 0.154 | 0.840 | 0.646 |
| 0.007 | 0.000 | 0.993 | 0.972 |

| $\beta_1$ | $\beta_2$ | $\beta_3$ | $\theta$ |
|---|---|---|---|
| 1.000 | 0.000 | 0.000 | 1.000 |
| 1.000 | 0.000 | 0.000 | 1.000 |
| 1.000 | 0.000 | 0.000 | 1.000 |
| 1.000 | 0.000 | 0.000 | 1.000 |
| 0.000 | 0.981 | 0.019 | 0.266 |
| 1.000 | 0.000 | 0.000 | 0.996 |
| 0.998 | 0.000 | 0.002 | 0.001 |
| 1.000 | 0.000 | 0.000 | 1.000 |
| 0.000 | 0.999 | 0.001 | 0.998 |
| 0.000 | 0.020 | 0.980 | 0.894 |
| 0.003 | 0.206 | 0.791 | 0.547 |
| 0.008 | 0.000 | 0.992 | 0.965 |

should be considered. First, under the condition that a reasonable prediction accuracy of the model can be achieved, we should use as few antecedent attributes and referential points as possible to keep the BRB model concise. For example, only Pb is selected as the antecedent attribute of the BRB subsystem for the main bearing and only two referential points are used for Fe in the BRB subsystem for lubricating oil. Second, when ignorance exists in the BRB expert system, more information should be added into the antecedent attributes to eliminate or reduce the ignorance of the BRB expert system. If the ignorance of the BRB expert system cannot be eliminated, it should be considered to avoid the model giving a misleading or totally wrong result as what we did in the construction of the BRB subsystems for cylinder liner-piston ring and lubricating oil.

The application of the optimized BRB expert system to abnormal wear detection verified the effectiveness of the fault diagnostic model we proposed in this paper. The results given by the optimized BRB expert system are better than those given by the ANN models and SVM models. We have also shown that the binary logistic regression modeling technique is not feasible when data distributes at either normal or abnormal end. It is important to note that the structure of the BRB expert system does not change and its parameters change only slightly when different training datasets are used to build the model. This shows that the optimized BRB expert system is more stable and credible than the ANN models and SVM models. We have shown that the structures and parameters of best performing ANN models can be different when different datasets are used for training the models.

By using a historical spectral data in 1000-h reliability test of a four-stroke diesel engine, we further tested the effectiveness of the optimized BRB expert system for fault diagnosis of a marine diesel engine, and the result is also promising, indicating that the BRB fault diagnostic model with the new structure can be well applied in fault diagnosis of marine diesel engines.

Although the wear fault of main bearing is well identified, the capability of this model needs to be verified using more data collected from real world operations of different marine diesel engines. Meanwhile, more representative samples should be used to optimize this system to increase its credibility and reliability. Additionally, we will take more measures to eliminate or reduce the ignorance of the BRB expert system in the future. Specifically, more real data samples on different wear faults will be accumulated, experiments will be conducted on testing engines to explore the relationship between fault features and fault modes, especially the multiple fault modes, and multisource information, such as vibration signals and the number of wear particles will be combined with oil information to detect wear faults of marine diesel engines more accurately.

The way the BRB expert system is developed in this paper can also be applied in other fault diagnosis especially when multiple faults co-exist. The issues considered in the construction of the proposed model, such as how to decide the numbers of antecedent attributes and their referential points, and how to eliminate the ignorance of the model as much as possible are also useful for building BRB models in various other data driven modeling and machine learning applications.

## APPENDIX

### A. Parameters of Each BRB Subsystem Trained by Different Training Datasets

*1) BRB Subsystem for Piston:*

$$\delta : \begin{bmatrix} 1 & 1 & 1 & 1 & 1 \end{bmatrix}$$

$$\begin{matrix} \beta_1 & \beta_2 & \theta \end{matrix} \quad \begin{matrix} \beta_1 & \beta_2 & \theta \end{matrix} \quad \begin{matrix} \beta_1 & \beta_2 & \theta \end{matrix}$$

$$\begin{bmatrix} 1 & 0 & 1 \\ 0 & 1 & 0.938 \end{bmatrix} \begin{bmatrix} 1 & 0 & 1 \\ 0 & 1 & 0.971 \end{bmatrix} \begin{bmatrix} 1 & 0 & 0.999 \\ 0 & 1 & 0.905 \end{bmatrix}$$

$$\begin{matrix} \beta_1 & \beta_2 & \theta \end{matrix} \quad \begin{matrix} \beta_1 & \beta_2 & \theta \end{matrix}$$

$$\begin{bmatrix} 1 & 0 & 1 \\ 0 & 1 & 0.945 \end{bmatrix} \begin{bmatrix} 1 & 0 & 1 \\ 0 & 1 & 0.958 \end{bmatrix}.$$

*2) BRB Subsystem for Main Bearing:*

$$\delta : \begin{bmatrix} 1 & 1 & 1 & 1 & 1 \end{bmatrix}$$

$$\begin{matrix} \beta_1 & \beta_2 & \theta \end{matrix} \quad \begin{matrix} \beta_1 & \beta_2 & \theta \end{matrix}$$

$$\begin{bmatrix} 1 & 0 & 1 \\ 0.347 & 0.653 & 0.001 \\ 0 & 1 & 1 \end{bmatrix} \begin{bmatrix} 1 & 0 & 1 \\ 0.289 & 0.711 & 0.001 \\ 0 & 1 & 1 \end{bmatrix}$$

$$\begin{matrix} \beta_1 & \beta_2 & \theta \end{matrix} \quad \begin{matrix} \beta_1 & \beta_2 & \theta \end{matrix}$$

$$\begin{bmatrix} 1 & 0 & 1 \\ 0.31 & 0.69 & 0.001 \\ 0 & 1 & 1 \end{bmatrix} \begin{bmatrix} 1 & 0 & 1 \\ 0.31 & 0.69 & 0.001 \\ 0 & 1 & 1 \end{bmatrix}$$

$$\begin{matrix} \beta_1 & \beta_2 & \theta \end{matrix}$$

$$\begin{bmatrix} 1 & 0 & 1 \\ 0.297 & 0.703 & 0.001 \\ 0 & 1 & 1 \end{bmatrix}.$$

*3) BRB Subsystem for Cylinder Liner-Piston Ring:* Refer equation at the top of p. 14.

*4) BRB Subsystem for Lubricating Oil:* Refer equation at the top of p. 15.

## ACKNOWLEDGMENT

The authors would like to thank the anonymous referees for their helpful comments and suggestions.

## REFERENCES

[1] L. A. Malm, J. Enström, and A. Hultman, "Main engine damage study," The Swedish Club, Gothenburg, Sweden, Tech. Rep., 2012. [Online]. Available: http://www.eyemag.se/core/main.php?SITEID=a43e8&PROJECTNR=4709

[2] R. K. Autar, "An automated diagnostic expert system for diesel engines," *J. Eng. Gas Turbines Power*, vol. 118, no. 3, pp. 673–679, 1996.

[3] S. Cebi, M. Celik, C. Kahraman, and I. D. Er, "An expert system towards solving ship auxiliary machinery troubleshooting: SHIPAMTSOLVER," *Expert Syst. Appl.*, vol. 36, no. 3, pp. 7219–7227, 2009.

[4] Z. X. Peng and S. Goodwin, "Wear-debris analysis in expert systems," *Tribol. Lett.*, vol. 11, nos. 3–4, pp. 177–184, 2001.

[5] P. W. Tse, E. Y. Li, J. C. Chan, and J. T. Leung, "Automatic generator health assessment system that embedded with advanced fault diagnosis and expert system," in *Proc. Prognostics Syst. Health*, Macao, China, 2010, pp. 1–7.

[6] O. C. Basurko and Z. Uriondo, "Condition-based maintenance for medium speed diesel engines used in vessels in operation," *Appl. Thermal Eng.*, vol. 80, pp. 404–412, Apr. 2015.

[7] F. Cruz-Peragon, F. J. Jimenez-Espadafor, J. M. Palomar, and M. P. Dorado, "Combustion faults diagnosis in internal combustion engines using angular speed measurements and artificial neural networks," *Energy Fuel*, vol. 22, no. 5, pp. 2972–2980, 2008.

[8] Z. W. Guo, C. Q. Yuan, Z. X. Li, Z. X. Peng, and X. P. Yan, "Condition identification of the cylinder liner-piston ring in a marine diesel engine using bispectrum analysis and artificial neural networks," *Insight Non Destruct.*, vol. 55, no. 11, pp. 621–626, 2013.

[9] H.-H. Tsai and C.-Y. Tseng, "Detecting solenoid valve deterioration in in-use electronic diesel fuel injection control systems," *Sensors*, vol. 10, no. 8, pp. 7157–7169, 2010.

[10] J.-D. Wu and C.-H. Liu, "An expert system for fault diagnosis in internal combustion engines using wavelet packet transform and neural network," *Expert Syst. Appl.*, vol. 36, no. 3, pp. 4278–4286, 2009.

[11] C. Szegedy *et al.*, "Intriguing properties of neural networks," *arXiv preprint arXiv:1312.6199*, 2013. [Online]. Available: http://arxiv.org/pdf/1312.6199v4.pdf

[12] N. Murata, S. Yoshizawa, and S. I. Amari, "Network information criterion-determining the number of hidden units for an artificial neural network model," *IEEE Trans. Neural Netw.*, vol. 5, no. 6, pp. 865–872, Nov. 1994.

[13] Z. X. Li, X. P. Yan, C. Q. Yuan, and Z. X. Peng, "Intelligent fault diagnosis method for marine diesel engines using instantaneous angular speed," *J. Mech. Sci. Technol.*, vol. 26, no. 8, pp. 2413–2423, 2012.

[14] S. W. Chen, Z. G. Li, and Q. S. Xu, "Grey target theory based equipment condition monitoring and wear mode recognition," *Wear*, vol. 260, nos. 4–5, pp. 438–449, 2006.

[15] J. Z. Vasu, A. K. Deb, and S. Mukhopadhyay, "MVEM-based fault diagnosis of automotive engines using Dempster–Shafer theory and multiple hypotheses testing," *IEEE Trans. Syst., Man, Cybern., Syst.*, vol. 45, no. 7, pp. 977–989, Jul. 2015.

[16] D. Antory, "Application of a data-driven monitoring technique to diagnose air leaks in an automotive diesel engine: A case study," *Mech. Syst. Signal Process.*, vol. 21, no. 2, pp. 795–808, 2007.

[17] D.-L. Xu *et al.*, "Inference and learning methodology of belief-rule-based expert system for pipeline leak detection," *Expert Syst. Appl.*, vol. 32, no. 1, pp. 103–113, 2007.

[18] J.-B. Yang, J. Liu, J. Wang, H.-S. Sii, and H.-W. Wang, "Belief rule-base inference methodology using the evidential reasoning approach—RIMER," *IEEE Trans. Syst., Man, Cybern. A, Syst., Humans*, vol. 36, no. 2, pp. 266–285, Mar. 2006.

[19] J.-B. Yang, J. Liu, D.-L. Xu, J. Wang, and H. Wang, "Optimization models for training belief-rule-based systems," *IEEE Trans. Syst., Man, Cybern. A, Syst., Humans*, vol. 37, no. 4, pp. 569–585, Jul. 2007.

[20] Z.-J. Zhou, C.-H. Hu, J.-B. Yang, D.-L. Xu, and D.-H. Zhou, "Online updating belief-rule-base using the RIMER approach," *IEEE Trans. Syst., Man, Cybern. A, Syst., Humans*, vol. 41, no. 6, pp. 1225–1243, Nov. 2011.

[21] G. L. Kong, D.-L. Xu, X. B. Liu, and J.-B. Yang, "Applying a belief rule-base inference methodology to a guideline-based clinical decision support system," *Expert Syst.*, vol. 26, no. 5, pp. 391–408, 2009.

[22] Z.-J. Zhou, L.-L. Chang, C.-H. Hu, X.-X. Han, and Z.-G. Zhou, "A new BRB-ER-based model for assessing the lives of products using both failure data and expert knowledge," *IEEE Trans. Syst., Man, Cybern., Syst.*, vol. 46, no. 11, pp. 1529–1543, Nov. 2016.

[23] Y.-M. Wang, J.-B. Yang, D.-L. Xu, and K.-S. Chin, "Consumer preference prediction by using a hybrid evidential reasoning and belief rule-based methodology," *Expert Syst. Appl.*, vol. 36, no. 4, pp. 8421–8430, 2009.

[24] Y. F. Wang, M. Xie, K.-S. Chin, and X. J. Fu, "Accident analysis model based on Bayesian network and evidential reasoning approach," *J. Loss Prevent. Process Ind.*, vol. 26, no. 1, pp. 10–21, 2013.

[25] Z. L. Yang *et al.*, "Selection of techniques for reducing shipping NOx and SOx emissions," *Transp. Res. D Transp. Environ.*, vol. 17, no. 6, pp. 478–486, 2012.

[26] J. F. Zhang, X. P. Yan, D. Zhang, S. Haugen, and X. Yang, "Safety management performance assessment for maritime safety administration (MSA) by using generalized belief rule base methodology," *Safety Sci.*, vol. 63, pp. 157–167, Mar. 2014.

[27] X.-B. Xu, Y.-H. Wang, C.-L. Wen, X.-Y. Sun, and D.-L. Xu, "Track vertical irregularity detection based on inference of belief rule base," *J. Chin. Railway Soc.*, vol. 36, no. 12, pp. 70–78, 2014.

[28] X. Zhao, S. C. Wang, J. S. Zhang, Z. L. Fan, and H. B. Min, "Real-time fault detection method based on belief rule base for aircraft navigation system," *Chin. J. Aeronaut.*, vol. 26, no. 3, pp. 717–729, 2013.

[29] A. Kodali, K. Pattipati, and S. Singh, "Coupled factorial hidden markov models (CFHMM) for diagnosing multiple and coupled faults," *IEEE Trans. Syst., Man, Cybern., Syst.*, vol. 43, no. 3, pp. 522–534, May 2013.

[30] W. Zhang, C. P. Shi, C. H. Hu, and Z. J. Zhou, "Fault diagnosis of engine based on RIMER expert system," *Syst. Simulat. Technol.*, vol. 7, no. 1, pp. 11–15, 2011.

[31] O. Basir and X. H. Yuan, "Engine fault diagnosis based on multi-sensor information fusion using Dempster–Shafer evidence theory," *Inf. Fusion*, vol. 8, no. 4, pp. 379–386, 2007.

[32] M. Galar, A. Fernández, E. Barrenechea, H. Bustince, and F. Herrera, "An overview of ensemble methods for binary classifiers in multi-class problems: Experimental study on one-vs-one and one-vs-all schemes," *Pattern Recognit.*, vol. 44, no. 8, pp. 1761–1776, 2011.
[33] J.-B. Yang, "Rule and utility based evidential reasoning approach for multiattribute decision analysis under uncertainties," *Eur. J. Oper. Res.*, vol. 131, no. 1, pp. 31–61, 2001.
[34] X. P. Yan, C. X. Sheng, J. B. Zhao, K. Yang, and Z. X. Li, "Study of on-line condition monitoring and fault feature extraction for marine diesel engines based on tribological information," *Proc. Inst. Mech. Eng. O J. Risk Rel.*, vol. 229, no. 4, pp. 1–10, 2014.
[35] J.-W. Gao, P.-L. Zhang, Y.-T. Zhang, and G.-Q. Ren, "Study on wearing characteristics and diagnosis based on oil spectrum analysis," *Trans. CSICE*, vol. 22, no. 6, pp. 571–576, 2004.
[36] T. X. Chen, "Application of spectrometric analysis of lub oil for 8NVD48A-2U medium-speed marine diesel engine," *J. SSSRI*, vol. 13, no. 2, pp. 35–46, 1990.
[37] D.-C. Li, H.-C. Hsu, T.-I. Tsai, T.-J. Lu, and S. C. Hu, "A new method to help diagnose cancers for small sample size," *Expert Syst. Appl.*, vol. 33, no. 2, pp. 420–424, 2007.
[38] D.-C. Li, C.-S. Wu, T.-I. Tsai, and Y.-S. Lina, "Using mega-trend-diffusion and artificial samples in small data set learning for early flexible manufacturing system scheduling knowledge," *Comput. Oper. Res.*, vol. 34, no. 4, pp. 966–982, 2007.
[39] M. D. Ruopp, N. J. Perkins, B. W. Whitcomb, and E. F. Schisterman, "Youden index and optimal cut-point estimated from observations affected by a lower limit of detection," *Biometrical J.*, vol. 50, no. 3, pp. 419–430, 2008.
[40] T. Fawcett, "An introduction to ROC analysis," *Pattern Recognit. Lett.*, vol. 27, no. 8, pp. 861–874, 2006.
[41] W. J. Youden, "Index for rating diagnostic tests," *Cancer*, vol. 3, no. 1, pp. 32–35, 1950.
[42] Z.-G. Zhou *et al.*, "A bi-level belief rule based decision support system for diagnosis of lymph node metastasis in gastric cancer," *Knowl. Based Syst.*, vol. 54, pp. 128–136, Dec. 2013.
[43] L. M. Zhang, *Models and Applications of Artificial Neural Network*. Shanghai, China: Fudan Univ. Press, 1993, pp. 43–44.

**Xiaojian Xu** received the B.S. degree in energy and power engineering and the M.S. degree in marine engineering from the Wuhan University of Technology, Wuhan, China, in 2011 and 2014, respectively, where she is currently pursuing the Ph.D. degree with the Key Laboratory of Marine Power Engineering and Technology (Ministry of Transport), Reliability Engineering Institute, National Engineering Research Center for Water Transport Safety.

She is a joint Ph.D. student with the University of Manchester, Manchester, U.K., from 2016 and 2017. Her current research interests include condition monitoring and intelligent fault diagnosis of diesel engines.

**Xinping Yan** received the B.S. and M.S. degrees in marine mechanical engineering from the Wuhan University of Water Transportation Engineering, Wuhan, China, in 1982 and 1987, respectively, and the Ph.D. degree in mechanical engineering from Xi'an Jiaotong University, Xi'an, China, in 1997.

He is currently a Chair Professor in Transport Safety and Reliability Engineering, and the Director of National Engineering Research Center for Water Transport Safety, Wuhan University of Technology. He has published over 200 journal papers, book chapters, and conference papers. His current research interests include marine system design and control, condition monitoring and fault diagnosis, and tribology and safety.

**Chenxing Sheng** received the B.S., M.S., and Ph.D. degrees in vehicle operation engineering from the Wuhan University of Technology, Wuhan, China, in 1992, 2001, and 2009, respectively.

He is currently a Professor with the Key Laboratory of Marine Power Engineering and Technology (Ministry of Transport), Reliability Engineering Institute, National Engineering Research Center for Water Transport Safety, Wuhan University of Technology. His current research interests include condition monitoring and fault diagnosis of diesel engine.

**Chengqing Yuan** received the B.S. degree in chemical engineering from Wuhan Automobile Polytechnic University, Wuhan, China, in 1998, the M.S. degree in mechanical design and theory from the Wuhan Research Institute of Material Protection, Wuhan, in 2001, and the Ph.D. degree in vehicle operation engineering from the Wuhan University of Technology, Wuhan, in 2005.

He is currently a Professor with the Key Laboratory of Marine Power Engineering and Technology (Ministry of Transport), Reliability Engineering Institute, National Engineering Research Center for Water Transport Safety, Wuhan University of Technology. He has published 34 SCI papers and over 60 EI papers. His current research interests include reliability and green technologies of marine power system.

**Dongling Xu** received the B.Eng. degree in electrical engineering from Hunan University, Changsha, China, in 1983 and the M.Eng. and Ph.D. degrees in system control engineering from Shanghai Jiao Tong University, Shanghai, China, in 1986 and 1988, respectively.

She is a Professor of decision sciences and systems with Alliance Manchester Business School, University of Manchester, Manchester, U.K. She has developed several interactive Web-based decision support tools, windows-based intelligent decision systems (IDS), and fault detection systems. Those systems are used in a wide range of assessment and decision making activities by organizations, such as General Motors, Detroit, MI, USA, Tesco, Welwyn Garden City, U.K., NHS, London, U.K., Ford, Dearborn, MI, USA, Shell, London, BP, London, and CNOOC, Beijing, China, in areas, such as safety and risk assessment, organizational self-assessment in quality management, policy assessment, and pipeline leak detection. The IDS software is used by practitioners and researchers from over 50 countries in the world. She has published over 150 peer reviewed journal papers, book chapters, and conference papers. Her current research interests include multiple criteria and multiple objective decision modeling, analysis and support under uncertainty, complex system and process modeling, and statistical fault detection and system development.

Ms. Xu currently serves as an Associate Editor for the *International Journal of Automation and Computing*, and the *International Journal of Computational Intelligence Systems*. She has been a conference co-chair or a program committee member for several international conferences.

**Jianbo Yang** received the B.Eng. and M.Eng. degrees in control engineering from North Western Polytechnic University, Xi'an, China, in 1981 and 1984, respectively, and the Ph.D. degree in systems engineering from Shanghai Jiao Tong University, Shanghai, China, in 1987.

He is a Professor of decision and system sciences and the Director of the Decision and Cognitive Sciences Research Centre, Alliance Manchester Business School, University of Manchester, Manchester, U.K. He is also a Specially Appointed Changjiang Chair Professor with the School of Management, Hefei University of Technology, Hefei, China. In the past three decades, he has been conducting research in evidential reasoning theory, multiple criteria decision analysis under uncertainty, multiple objective optimization, intelligent decision support systems, hybrid quantitative and qualitative decision modeling using techniques from operational research, artificial intelligence and systems engineering, system modeling, and simulation and control for engineering and management systems. He has published four books, over 180 journal papers and book chapters, and a similar number of conference papers, and developed several software packages including the Windows-based intelligent decision system via evidential reasoning. His current research has been supported by Engineering and Physical Science Research Council, European Commission, Department for Environment Food & Rural Affairs, Science and Engineering Research Council, Hong Kong Research Grants Council, National Nature Science Foundation of China, and industry. His current research interests include financial decision-making, aggregated production management, maintenance management, risk and security modeling and analysis, quality modeling and evaluation, and the integrated evaluation of products, systems, projects, and policies.